EARTH SURFACE PROCESSES AND LANDFORMS
Earth Surf. Process. Landforms **42**, 128–156 (2017)

Published online 9 November 2016 in Wiley Online Library
(wileyonlinelibrary.com) DOI: 10.1002/esp.4052

State of Science

Controls on deep critical zone architecture: a historical review and four testable hypotheses

Clifford S. Riebe,[1]* W. Jesse Hahm[1,2] and Susan L. Brantley[3]
[1] Department of Geology and Geophysics, University of Wyoming, Laramie, WY USA
[2] Department of Earth and Planetary Science, University of California, Berkeley, CA USA
[3] Department of Geosciences and the Earth and Environmental Systems Institute, Pennsylvania State University, University Park, PA USA

Received 31 August 2016; Revised 7 September 2016; Accepted 7 September 2016

*Correspondence to: Clifford S. Riebe, Department of Geology and Geophysics, University of Wyoming, Laramie, WY 82071, USA. E-mail: criebe@uwyo.edu

ESPL
Earth Surface Processes and Landforms

ABSTRACT: The base of Earth's critical zone (CZ) is commonly shielded from study by many meters of overlying rock and regolith. Though deep CZ processes may seem far removed from the surface, they are vital in shaping it, preparing rock for infusion into the biosphere and breaking Earth materials down for transport across landscapes. This special issue highlights outstanding challenges and recent advances of deep CZ research in a series of articles that we introduce here in the context of relevant literature dating back to the 1500s. Building on several contributions to the special issue, we highlight four exciting new hypotheses about factors that drive deep CZ weathering and thus influence the evolution of life-sustaining CZ architecture. These hypotheses have emerged from recently developed process-based models of subsurface phenomena including: fracturing related to subsurface stress fields; weathering related to drainage of bedrock under hydraulic head gradients; rock damage from frost cracking due to subsurface temperature gradients; and mineral reactions with reactive fluids in subsurface chemical potential gradients. The models predict distinct patterns of subsurface weathering and CZ thickness that can be compared with observations from drilling, sampling and geophysical imaging. We synthesize the four hypotheses into an overarching conceptual model of fracturing and weathering that occurs as Earth materials are exhumed to the surface across subsurface gradients in stress, hydraulic head, temperature, and chemical potential. We conclude with a call for a coordinated measurement campaign designed to comprehensively test the four hypotheses across a range of climatic, tectonic and geologic conditions. Copyright © 2016 John Wiley & Sons, Ltd.

KEYWORDS: regolith production; near-surface geophysics; weathering; fractures

Introduction

Understanding connections between Earth's surface and subsurface processes is important in many cross-disciplinary problems, from assessing soil and water sustainability over human lifetimes (e.g. Richter *et al.*, 1994; Montgomery, 2007) to understanding weathering-climate feedbacks that integrate across the globe over millions of years (Walker *et al.*, 1981; Raymo and Ruddiman, 1992; Zhang *et al.*, 2001; Maher and Chamberlain, 2014). Increasingly, these problems are being tackled in innovative studies of the 'critical zone' (CZ) – the near-surface layer where water, rock, air and life meet in a dynamic interplay that sculpts landscapes, generates soils and builds the foundation for Earth's terrestrial ecosystems (National Research Council [NRC], 2001; Brantley *et al.*, 2006, 2007a; Anderson *et al.*, 2007; Chorover *et al.*, 2007). As the interface between air and rock, the CZ was originally defined to extend from the upper limits of vegetation to the lower limits of groundwater (NRC, 2001; Brantley *et al.*, 2006). Thus it integrates diverse processes, including the photosynthetic drawdown of atmospheric carbon into vegetation, its return to the atmosphere in respiration, and both the biotic and abiotic breakdown of soil and rock in the subsurface.

The zone of weathered rock can be tens to hundreds of meters thick (Ruxton and Berry, 1957, 1959; Thomas, 1966; Pavich, 1986; Ollier, 1988; Hubbert *et al.*, 2001; Anderson *et al.*, 2002; Dethier and Lazarus, 2006; Burke *et al.*, 2009). Yet the zone below the upper 1–2 m at Earth's surface has received relatively little attention in the literature, in part because the deeper subsurface is difficult to access and sample (see for example, collections edited by Cremeens *et al.*, [1994] and Zanner and Graham [2005]). Overcoming this limitation is important, because deeper processes have profound implications for processes at the surface and for the overall function of the CZ. For example, deep weathering produces and modifies regolith, generates flowpaths and storage space for water, and promotes ecosystem productivity by liberating life-sustaining nutrients from minerals in rock and regolith (e.g. Arkley 1981; Graham *et al.*, 1994). In many respects, subsurface weathering can be thought of as the inception of surface processes; it

prepares rock for infusion into the biosphere and subsequent transport as sediment across the landscape. Hence, study of the deep CZ is an important mutual frontier in geomorphology, low-temperature geochemistry, pedology, geobiology, terrestrial ecology and hydrology.

Although the deep CZ remains largely unexplored, innovative field and modeling applications of geophysics (Robinson *et al.*, 2008; Slim *et al.*, 2015; St Clair *et al.*, 2015; Parsekian *et al.*, 2015), geochemistry (Brantley and Lebedeva, 2011), hydrology (Salve *et al.*, 2012), soil science (Rasmussen *et al.*, 2011a), ecology (Phillips, 2009), and geomorphology (Pelletier *et al.*, 2013; Anderson *et al.*, 2013; Rempe and Dietrich, 2014) are increasingly contributing to process-based understanding of the subsurface. To highlight key challenges and recent advances of deep CZ research, we have edited this special issue on the topic for *Earth Surface Processes and Landforms* (ESPL). The contributed papers share the common goal of probing the deep CZ for an improved understanding of its form, function and evolution through the past and into the future. Here we briefly introduce these papers and discuss how they fit within the context of historical studies of CZ processes. We then outline a conceptual framework for understanding weathering in the deep CZ, building on four recently proposed hypotheses about how hydrology, weathering, erosion and tectonics influence deep CZ architecture.

Defining the Bottom of the CZ

Just how deep is 'deep' when we talk about the deep CZ? This is a non-trivial question (Richter and Markewitz 1995; Brantley *et al.*, 2011; West, 2012) in part because the answer should vary markedly from one place to the next, depending on a wide range of biological, geomorphic, geochemical and anthropogenic factors. Geologic factors, such as bedrock composition and landscape history (e.g. the advance and retreat of nearby ice) may be especially important in setting the overall thickness of the CZ. Here we limit our scope to defining the base of the CZ in landscapes with silicate bedrock, recognizing that a different definition is needed for carbonate landscapes, where a different style of weathering dominates.

As a starting point, we draw from the 2001 Basic Research Opportunities in Earth Sciences (BROES) report, in which the National Research Council (NRC) defined the CZ as 'the heterogeneous, near-surface environment in which complex interactions involving rock, soil, water, air, and living organisms regulate the natural habitat and determine the availability of life-sustaining resources' (NRC, 2001). Elsewhere in the report, the NRC clarified that this layer extends from the top of vegetation down 'through the pedosphere, unsaturated vadose zone, and saturated groundwater zone.' While this clearly pinpoints the top of the CZ, it is ambiguous and therefore unsatisfactory about defining the bottom.

To understand the problem with the BROES report's definition, it may help to imagine standing on a ridgetop and watching meteoric water as it percolates into the subsurface and flows through underlying Earth materials (Figure 1). Over a sufficiently long timescale, groundwater can circulate to great depths that do not necessarily correspond to any cutoff in the complex interactions referred to as CZ processes in the report. One way to overcome this limitation of the groundwater-based definition is to set the lower CZ boundary as the level where subsurface material grades into rock that is no longer affected by meteoric fluids (Brantley *et al.*, 2011). This is also problematic, however, because even pristine-seeming igneous bedrock can bear isotopic signatures of meteoric water (e.g. Taylor, 1974), reflecting the slow but inexorable movement of fluids through low-conductivity bedrock over geologic timescales.

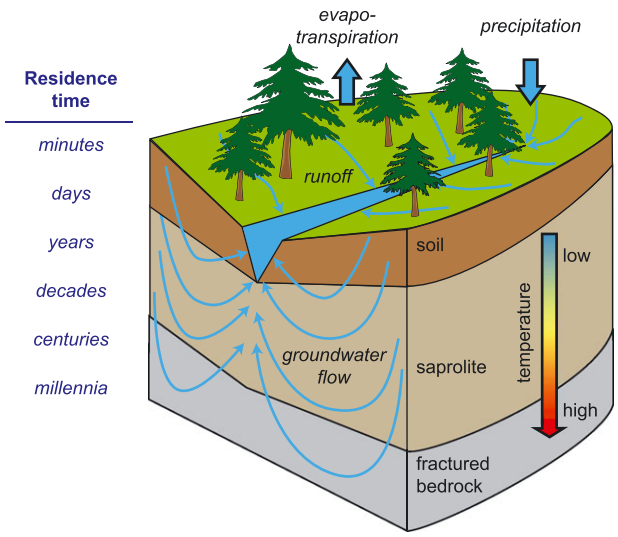

Figure 1. Schematic showing fluxes of water in the critical zone (CZ). The residence times of meteoric water vary from minutes for surface runoff to millennia for deeply circulating groundwater. Distinguishing between materials that are influenced by meteoric water and those that are not can be problematic. Thus, it may be more straightforward to identify the bottom of the CZ in terms of mineral assemblages and their equilibrium status relative to meteoric water (see Figure 2). [Colour figure can be viewed at wileyonlinelibrary.com]

An alternate definition of the lower limit of the CZ might be the depth at which temperatures rise to some specified level above ambient surface conditions (Figure 1). One could define such a temperature threshold as the depth at which groundwater grades into diagenetic water, which may or may not include meteoric water. Alternatively, the temperature threshold could be defined as the upper temperature limit on life, making the CZ the zone of continental lithosphere that contains biota (Brantley *et al.*, 2011). Either way, a temperature-based limit would overcome the inherent drawback of the groundwater-based limit. Yet there would still be at least one key problem: Landscapes in different regions of the world do not generally share the same thermal gradients with depth. In volcanic areas, for example, high temperatures found only at very deep depths in other landscapes may prevail at the land surface. Thus, although the surface is everywhere part of the CZ by definition, it might in some instances fail to fit within temperature-based limits that mark the base of the CZ in other landscapes. Specifying a temperature threshold for the base of the CZ is therefore problematic.

An equilibrium-based definition

The water- and temperature-based definitions discussed above are not entirely satisfactory. This leads us to a third definition, based on the depth of chemical equilibration between Earth materials and meteoric water in the subsurface (Figure 2). Here, equilibrium refers to a local condition that develops over some distance and time period that are both smaller than the scales of interest (Knapp, 1989).

To understand our equilibrium-based definition, it may help to imagine not only the downward movement of meteoric fluids over time (Figure 1), but also the upward, conveyor-like movement of solid materials through the subsurface (Figure 2). This CZ conveyor, which is colloquially known as the 'weathering engine' (Anderson *et al.*, 2004), is driven by erosion at the surface. In effect, surface lowering by erosion brings minerals upward from depth and thus exposes them increasingly to geophysical, geochemical and biological processes that can alter them (Figure 2).

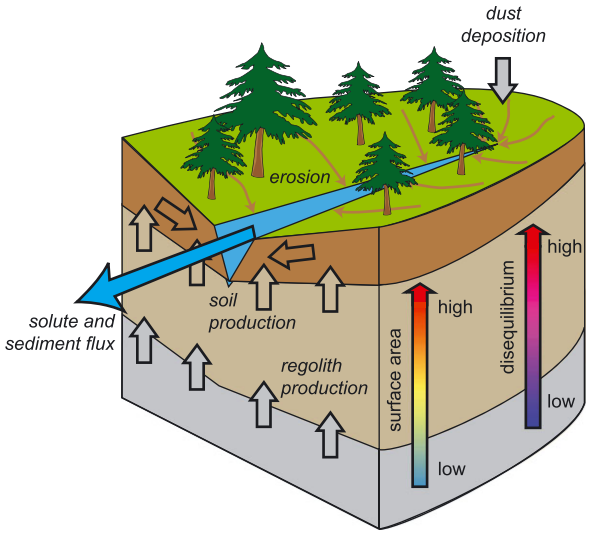

Figure 2. Schematic showing fluxes of Earth materials in the critical zone (CZ). Production of regolith from fractured but otherwise unweatherered bedrock (gray arrows) increases the surface area of weatherable minerals and exposes them to an increasing volume of reactive waters from the surface. Thus the degree of disequilibrium increases towards the surface. Conversion of saprolite to physically mobile soil (light brown arrows) promotes erosion (dark brown arrows), which lowers the surface. The overall process effectively carries rock material from depths – where fractures containing out-of-equilibrium water are sparse – to shallower levels – where fracturing is denser and minerals are thus increasingly exposed to reactive fluids. [Colour figure can be viewed at wileyonlinelibrary.com]

Beginning at some sufficiently deep depth, water circulates slowly enough relative to the upward advection of Earth materials that it chemically equilibrates with the surrounding mineral assemblage. Here, the delivery of meteoric reactants (mainly H_2O, CO_2, O_2) is slow, and the area of mineral surfaces that are exposed to meteoric fluids (A_f) is high relative to the volume of reactive fluid (V_f) that flows past a given unit of mineral surface per unit time. Isotopic alteration is possible at these depths due to the slow but inexorable passage of meteoric fluids through interconnected pores (Lee *et al.*, 1991), but fluid chemistry is nonetheless dominated by rock chemistry, and minerals show little-to-no alteration in bulk geochemistry relative to minerals in bedrock. Here, chemical equilibrium is generally maintained throughout the system, and the complex interactions that define CZ processes according to the BROES report are either absent or operate very slowly.

As the weathering engine exhumes minerals to shallower depths along the conveyor, they eventually cross into the CZ. At this lower boundary of the CZ, the chemical equilibrium that dominated at greater depths gives way to the complex interactions that are the hallmarks of the CZ according to the BROES report (NRC, 2001). Here, fluids are flowing quickly enough to measurably affect solid phases in both their isotopes and their bulk chemistry. Chemical weathering reactions begin forming new lower-temperature, lower-pressure mineral assemblages. Solutes are released, liberating vital nutrients for use in the terrestrial ecosystem. These reactions are possible because the average A_f/V_f ratio of the mineral-fluid system changes as minerals rise to the surface, reflecting an increase in flow of reactants through fracture networks that outpaces any concurrent increases in mineral surface (Figures 1 and 2).

Where rock meets life?

As the interface between air and rock, the CZ responds to ambient conditions at Earth's surface, including changes in climate and anthropogenic activity. Changes at the land surface and processes in the deep CZ are ultimately linked by the development of high-conductivity flow pathways for meteoric fluids and biota. Because the deep CZ is a zone where silicate mineral assemblages show measurable changes that approach a new chemical equilibrium with the biota-rich surface environment (Brantley *et al.*, 2011), it is characterized by gradients that can be harnessed by diverse communities of organisms who survive via the catalysis of chemical reactions (Banfield *et al.*, 1999). In this context, our equilibrium-based definition of the base of the CZ is broadly consistent with the conceptual view of the CZ as the zone where rock meets life (Brantley *et al.*, 2007b). However, the ongoing revolution in microbial community genomics (e.g. Hug *et al.*, 2016) holds promise that researchers will identify metabolic strategies that microbes employ below depths where pore fluids are essentially in equilibrium with rock. The finding of new life many kilometers beneath Earth's surface may therefore pose a contradiction between our equilibrium-based definition and the original rock-meets-life conception of the thickness of the critical zone.

Going Back through Time to Understand the Deep CZ

Because the CZ is the interface of high-temperature rocks at depth and surficial conditions at Earth's surface, it harbors considerable gradients in fluid chemistry, bulk geochemistry, mineral assemblages, mineral surface area, porosity, and biota. Over the years, these CZ gradients have been measured and studied in many different settings in remarkable detail, revealing evidence of past CZ processes and providing information that we can use to forecast the future of CZ services. This forecasting, referred to colloquially as 'Earth-casting' (Goddéris and Brantley, 2014), is a major thrust of CZ science, which unites other watershed-centric sciences in its emphasis on crossing disciplines and timescales (Brantley *et al.*, 2007a). Thus, while geomorphologists, ecologists, pedologists, geochemists and geobiologists alike have been studying gradients in the CZ to various disciplinary ends for centuries, the relatively new and integrative field of CZ science is seeking more than ever to combine observations across disciplines for a comprehensive, quantitative understanding of CZ evolution over a wide range of spatiotemporal scales (Brantley *et al.*, 2007a). It is therefore appropriate that we review the major developments throughout history in understanding the evolution of the CZ. Thus we provide context for this special issue's contributions, which are introduced along the way. In this review, we focus much of our attention on advances that have emerged from studies of hilly and mountainous terrain, where erosion at the surface exhumes Earth materials from depth along a trajectory that exposes them increasingly to reactive fluids and biota from the surface (as illustrated in Figures 1 and 2). In these landscapes, what happens at depth does not stay at depth, so understanding deep CZ processes is highly relevant to understanding surface and near-surface processes.

Observations of the deep CZ

Perhaps one of the first scientists to delve into at least the upper part of the deep CZ was Bernard Palissy, a potter in France who wrote about the use of *la tarière* (the auger) to bore into the Earth:

> I can advise you as to no more expedient a method than that I should use myself ... I should drill and bore away with the

> full length of the whole handle at all the ditches in my estate ... I should determine the nature of the deepest layers; and ... I should bore all over the fields ... in many a place the rocks are soft and tender, especially when they are planted in the ground.

This translation is based on texts he published in 1563 and 1580 (after Feller *et al.*, 2006).

Today, CZ scientists still use augers and other boring devices to gather information about the subsurface. For example, one contribution to this special issue (Holbrook *et al.*, 2014) includes an investigation of subsurface porosity and water content based on samples collected with a hand auger in the Sierra Nevada, California. Another (Buss *et al.*, 2013) reports an investigation of subsurface weathering and fracturing in the Bisley Watershed, Puerto Rico, based on cores from boreholes that were wireline-drilled to depths of 27 and 37 m. This far exceeds the depths that Palissy reached with his auger in the mid-1500s.

By 1763, soil horizons in pits and other excavations were being delineated and described in remarkable detail in terms of process by another Frenchman, Georges-Louis Leclerc de Buffon (Feller *et al.*, 2006). Today, CZ scientists exploit boreholes, roadcuts and, increasingly, geophysical methods to delimit horizons, reaction fronts and fracturing in the subsurface. For example, one paper in this special issue (Slim *et al.*, 2015) features downhole logging of fractures in a series of boreholes at the Shale Hills Critical Zone Observatory (CZO). Data on fractures from these boreholes were compared to predictions from a model of topographic and tectonic stresses, which together induce a subsurface stress field that may often be vital to opening fractures and thus delivering meteoric water and biota to the base of the CZ (Slim *et al.*, 2015; St. Clair *et al.*, 2015). This special issue also includes a report on gradients in weathering across a climosequence in Hawaii; a key finding from the roadcuts and beach–cliff exposures of weathered basalt was that the distribution of regolith thickness is highly variable and appears to be connected with the local moisture balance of the landscape (Goodfellow *et al.*, 2014). This special issue also includes reports from two geophysical studies of deep CZ architecture. In one of them, resistivity data from the Boulder Creek CZO provided evidence for substantial variability across slopes in regolith properties at depth (Leopold *et al.*, 2013). In the other study, a coupled analysis of resistivity and seismic refraction data from the Southern Sierra CZO was used to delimit water flowpaths and gradients in porosity in the deep subsurface (Holbrook *et al.*, 2014).

In the late 1700s, due to the absence of modern borehole logging and geophysical tools, researchers like de Buffon were stuck describing soil horizons in excavations that could be accessed with augers and shovels. Around the same time, James Hutton, a Scotsman, began to argue for what is now known as the theory of uniformitarianism (Hutton, 1788). In his 1788 classic, Hutton famously wrote,

> The ruins of an older world are visible in the present structure of our planet; and the strata which now compose our continents have been once beneath the sea, and were formed out of the waste of preexisting continents. The same forces are still destroying, by chemical decomposition or mechanical violence, even the hardest rocks and transporting the materials to the sea ... .

Thus, in a single succinct and oft-quoted statement, Hutton highlighted the importance of the as-yet-unnamed field of CZ science in understanding Earth's history. Moreover, Hutton's argument, that the present is the key to the past, implicitly projects forwards as well as backwards, highlighting the importance of understanding processes at work both today and in the past in order to realistically Earth-cast the evolution of the CZ into the future.

Studies of weathering reactions

By the mid-1800s, chemical weathering was being attributed to the action of water plus carbonic acid (Fournet, 1833; Hartt, 1853). This idea became more quantitative following the work of the American brothers William and Robert Rogers, who recorded observations of the reactions of powdered minerals, including feldspars, mica and analcime in the presence of carbonic acid (Rogers and Rogers, 1848). Later, in 1863, in his textbook titled 'Lehrbuch der chemischen und physikalischen Geologie', Gustav Bischof, of the University of Bonn in Germany, discussed how he used experimental data to calculate perhaps the first realistic estimate of the timescale of mineral weathering. He gauged that it would take more than six million years to completely dissolve 40 grains of hornblende in water and carbonic acid (Bischof, 1863). He also implicitly invoked the concept of interface-limited mineral weathering (formalized more than 100 years later by Berner, 1978) when he stressed the need for constant renewal of the water and acid solution in his hypothetical long-term dissolution experiment.

Shortly after Bischof's book was published, researchers were making the connection between the great span of time involved in weathering and the possible influence of past climates on weathering profiles. For example, the American T. Sterry Hunt (1874) argued that soil profiles in the Blue Ridge Mountains of Virginia were developed 'at a time when a highly carbonated atmosphere, and a climate very different from our own, prevailed.' Today, the great antiquity of very thick weathering profiles, particularly in cratonic settings in Brazil and Australia (Nahon, 1986; Ollier, 1988; Vasconcelos *et al.*, 1994; Vasconcelos and Conroy, 2003), can be quantified using modern dating techniques, such as $^{40}Ar/^{39}Ar$ geochronology and (U-Th)/He dating of secondary minerals (Shuster *et al.*, 2005; Li *et al.*, 2007; Shuster *et al.*, 2012). In this special issue of ESPL, the great depths of weathering and modest erosion rates reported in two studies imply long legacies of past environments on weathering profiles developed in the Sierra Nevada, California (Holbrook *et al.*, 2014), and in the mountains of Puerto Rico (Buss *et al.*, 2013). In a recent study of the influence of Pleistocene climate on paleo-erosion rates in the Oregon Coast Ranges, Marshall *et al.* (2015) have suggested that peri-glacial processes during past climates may have widespread implications for interpreting observations of the CZ.

In the mid to late 1800s, around the same time that the importance of carbonic acid was being recognized, at least one scientist, Alexandre Brongniart, at the École des Mines in Paris, France, was arguing that electrical currents between different rock types were responsible for the decomposition of feldspar and the formation of kaolinite in granite (Galvez and Gaillardet, 2012). Although electrical currents are no longer considered to be the root of clay formation, the importance of redox reactions in general was recognized early and remains a focus today. For example, in 1840, Charles Jackson wrote,

> When a rock contains iron, or manganese, in a low state of oxidation, by exposure to air and moisture, those oxides attract more oxygen, and increase in bulk so as to cause the rock to cleave into thin layers, which are hove off by the agency of freezing water, or are worn off by friction and by the currents of brooks and rivers. (Jackson, 1840)

The importance of redox reactions in weathering within the deep CZ is highlighted in two contributions to this issue (Brantley *et al.*, 2013; Buss *et al.*, 2013).

Soon after Jackson described redox weathering of iron and manganese, the French mining engineer, Jacques-Joseph Ebelmen (1845) described in schematic form the reactions involved in silicate weathering, photosynthesis, and pyrite oxidation (Berner, 2012):

$$CO_2 + (Ca, Mg)SiO_3 \Leftrightarrow (Ca, Mg)CO_3 + SiO_2 \quad (1)$$

$$CO_2 + H_2O \Leftrightarrow CH_2O + O_2 \quad (2)$$

$$15O_2 + 4FeS_2 + 8H_2O \Leftrightarrow 2Fe_2O_3 + 8SO_4^{2-} + 16H^+ \quad (3)$$

Thus, Ebelmen laid the foundation for understanding connections between life and weathering under oxidizing conditions at the interface between air and rock (Berner, 2012; Galvez and Gaillardet, 2012), in what we now refer to as the CZ. In describing these reactions, Ebelman recognized that roots and organic acids from plants promote weathering. He also understood that silicate weathering could influence the concentration of carbon dioxide in the atmosphere (Berner *et al.*, 2003), a connection that is recognized today to be part of a vital thermostat for Earth's long history of habitable conditions (e.g. Walker *et al.*, 1981).

The important influence of vegetation on weathering was more broadly recognized and accepted as European researchers began to investigate the tropics. For example, Thomas Belt, an Englishman, wrote that the most intense weathering in Nicaragua occurred under forests due to 'percolation through rocks of rain water charged with a little acid from decomposing vegetation' (Belt, 1874). Today, connections between biota, weathering and landscape evolution are an area of vigorous research (Dietrich and Perron, 2006; Roering *et al.*, 2010; Brantley *et al.*, 2011; Hahm *et al.*, 2014) at the heart of understanding connections between the surface and the deep CZ (Brantley *et al.*, 2007b).

Studies of erosion, weathering and soil development

The turn of the twentieth century was a period of particularly rapid and overlapping intellectual advances in soil science and geomorphology. Charles Darwin (1876) described laterites, soil layering, and stone lines in one of a series of reports about his famous voyage on the HMS Beagle, laying the groundwork for the now flourishing field of understanding soils as integrated, constantly evolving biomantles (Johnson *et al.*, 2005). By 1895, the term 'saprolite' was being used to refer to the chemically altered but physically intact bedrock that underlies mobile or bioturbated soil (Becker, 1895). Today, saprolite is widely recognized as crucial to ecosystem function, pedogenic activity and the hydrologic cycle (Graham *et al.*, 2010), particularly in arid to semi-arid mountainous terrain, where it provides a vital reservoir of water in the dry season and times of drought (Arkley 1981; Dethier and Lazarus, 2006; Graham *et al.*, 2010; Bales *et al.*, 2011; Goulden *et al.*, 2012; Salve *et al.*, 2012). In this special issue, the importance of saprolite in surface processes was demonstrated in a geographic information system (GIS) investigation of the distribution and properties of saprolite in the coterminous United States (Wald *et al.*, 2013). According to the analyses conducted in that study, the top of saprolite often lies within 1 m of the land surface, especially in mountain states. This follows a long string of studies by Bob Graham, one of the study's coauthors, who has helped spotlight the vital importance of deep CZ processes in the development of overlying soils and the ecosystems they support (e.g. Jones and Graham, 1993; Graham *et al.*, 1994; Zanner and Graham, 2005; Graham *et al.*, 2010).

At about the same time that Darwin was writing about stone lines, Grove Karl Gilbert was engaged in what would eventually become a highly influential geological study of the Henry Mountains, in Utah. In his US Geological Survey report, Gilbert (1877) wrote perhaps the first description of the 'soil-production function' (Humphreys and Wilkinson, 2007) – i.e. the relationship between the rate of conversion of weathered rock to mobile regolith (now often called the soil-production rate) and the thickness of the mobile regolith (i.e. the soil):

> Solution and frost, the chief agents of rock decay, are both retarded by the excessive accumulation of disintegrated rock. Frost action ceases altogether at a few feet below the surface, and solution gradually decreases as the zone of its activity descends and the circulation on which it depends becomes more sluggish. Hence the rapid removal of the products of weathering stimulates its action, and especially that portion of its action which depends upon frost. If however the power of transportation is so great as to remove completely the products of weathering, the work of disintegration is thereby checked; for the soil which weathering tends to accumulate is a reservoir to catch rain as it reaches the earth and store it up for the work of solution and frost, instead of letting it run off at once unused.

Thus Gilbert described in qualitative terms a 'humped' relationship in which the soil production rate first increases with increasing thickness but then decreases after reaching a maximum rate at an intermediate soil thickness. In this framework, erosion of the landscape surface and the soil–bedrock interface are linked by the thickness of mobile regolith, which is ultimately determined by a feedback between soil production and erosion.

Gilbert (1909) also described the creep-like motion of regolith by freezing and thawing, heating and cooling, wetting and drying, and biotic activity in terms of landscape evolution, amplifying and elaborating on earlier writings by William Morris Davis (1892). To explain the ubiquity of convex drainage divides in badlands and hilly landscapes, Gilbert (1909) pointed out that there might be a tendency towards dynamic equilibrium, in which a stable convex form could be maintained under continuous erosion of the slope. In general, to maintain a stable topographic form, each point on a slope must transport not only the mobile regolith supplied by soil production from below, but also the material delivered by erosion from positions upslope of the point of interest. If the flux of eroded regolith can somehow increase systematically downslope, away from the drainage divide, the topographic form of the hillslope can be maintained in dynamic equilibrium. This could be accommodated on convex slopes by their characteristic downslope increase in hillslope gradients, if, according to Gilbert (1909), '… the impelling force, gravity, depends for its effectiveness on slope, being able to cause more rapid flow where the slope is steeper.' This might be generally true in gravity-driven, creep-like erosion along hillslopes (Gilbert, 1909). In Gilbert's (1909) redux of Davis' (1892) writings, 'the normal product of degradation by creep is a profile convex outward.' Evidently, Gilbert recognized that there might be a connection between process and form – that topographic curvature might both be set by and also help maintain the flux of sediment across slopes in a dynamic equilibrium. One way that soils can creep down slopes is through cyclical freezing and thawing of porewaters. One of the contributions to the special issue (Anderson *et al.*,

2013) highlights freezing as a mechanism for both the transport of material downslope and the conversion of bedrock to regolith due to damage that occurs when temperatures fall within the 'frost-cracking' window (−3 to −8 °C) of segregation ice growth (Walder and Hallet, 1985; Hales and Roering, 2005; Marshall *et al.*, 2015).

Collectively, in describing the transport of soil downslope due to variations in gradient, Davis (1892) and Gilbert (1877, 1909) had laid the conceptual foundations for the first 'geomorphic transport law' (Dietrich *et al.*, 2003). Moreover, they were the first to recognize and promote the idea that geomorphic processes might be expressed in landscapes through characteristic hillslope forms. Many of these ideas, including Gilbert's (1877) concept of the soil production function, went unnoticed or were simply forgotten for decades (Humphreys and Wilkinson, 2007). Yet they ultimately served as a crucial foundation of modern process geomorphology, which emerged in the second half of the twentieth century with renewed and increasingly quantitative interest in the concept of dynamic equilibrium (Hack, 1960), geomorphic transport laws (Culling, 1960; Dietrich *et al.*, 2003), and the soil production function (Ahnert, 1967; Carson and Kirkby, 1972). These concepts remain near the front of cutting edge research in geomorphology to this day (NRC, 2012). Moreover, understanding the production of altered material at the base of the CZ, under the collective mantle of overlying saprolite and soil, is a vital new frontier in process geomorphology (NRC, 2010; Lebedeva and Brantley, 2013; Anderson *et al.*, 2013; Rempe and Dietrich, 2014; Slim *et al.*, 2015; St Clair *et al.*, 2015).

As the nineteenth century ended, George Merrill (1897) published the first and second editions of a landmark book that summarized much of what was known at the time about rock weathering. This was also perhaps the first publication to report a calculation of mass loss from a soil using the enrichment of insoluble elements relative to their concentrations in parent bedrock (Amundson, 2014). In this precursor of modern solid-phase mass-balance studies of weathering, Merrill (1897) recognized that the enrichment of relatively insoluble elements such as iron and aluminum could put minimum constraints on losses of more soluble elements during the production and weathering of soils from bedrock. However, more than 40 years would pass before Samuel Goldich (1938) published his now-famous mineral stability series, and thus formalized the relative susceptibility of major rock-forming minerals to weathering at Earth's surface. Today, Merrill's insoluble-element approach is widely used to quantify weathering losses from soils in landscapes around the world (Nesbitt, 1979; Brimhall and Dietrich, 1987; Chadwick *et al.*, 1990; White, 1995; Riebe *et al.*, 2001b; White, 2008; White *et al.*, 2008; Dixon *et al.*, 2009; Ferrier *et al.*, 2011; Dixon *et al.*, 2012; Dixon and Riebe, 2014).

The foundations of modern soil science – which encompasses the formation of both soil and saprolite – were laid in the late 1800s, beginning with the work of Vasily Dokuchaev (as cited in Dokuchaev, 1967). However, it was not until the mid-1900s that Hans Jenny, who was strongly influenced by Dokuchaev (Amundson, 2014), developed and popularized the 'state-factor' approach to studying soil formation (Jenny, 1941). This approach recognizes the vital roles that climate, organisms, topography, parent material, and time all play in the evolution and observed state of soils. Teasing out the effects of any one factor therefore requires careful study design, in which sites are chosen to maximize the variation in the factor of interest and minimize the confounding effects of the other factors. The basis for studying climo-, eco-, topo-, litho-, and chrono-sequences of the CZ was born. Today, Jenny's state-factor approach underpins the experimental design of the CZOs (Anderson *et al.*, 2008), the Critical Zone Exploration Network (Brantley *et al.*, 2006), and the European CZO studies (Banwart *et al.*, 2011).

Input–output mass balance studies

Beginning in the late 1950s, studies of weathering became increasingly quantitative and focused on watershed-scale measurements. Anderson and Hawkes (1958) were perhaps the first to measure the relative mobility of major elements in streams draining small basins underlain by homogeneous bedrock. Soon thereafter, contributions of weathering to groundwater in the Sierra Nevada, California, were measured in outputs from springs (Feth *et al.*, 1964). Such fluxes were later evaluated in terms of weathering reactions using innovative inverse (Garrels and Mackenzie, 1967) and deterministic models (Pačes, 1973). At roughly the same time, it was recognized that precisely constrained budgets of cations in precipitation and stream water could be used to quantify weathering fluxes from small catchments (Likens *et al.*, 1967). The approach, which measures weathering fluxes as the difference between cation outputs in stream water and cation inputs in precipitation, was first applied at Hubbard Brook, in the north-eastern United States (Johnson *et al.*, 1968) and at Pond Branch, Maryland (Bricker *et al.*, 1968). The Pond Branch analysis compared chemical fluxes based on solutes with physical fluxes measured from a sediment trap (Bricker *et al.*, 1968), making it an early bridge between geochemistry and geomorphology and thus a vital precursor of modern CZ science.

By 1970, the uptake and release of solutes from biomass were explicitly included in mass-balance estimates of mineral weathering rates (Cleaves *et al.*, 1970). Catchment-scale studies of solutes proliferated during the 1970s and 1980s and were increasingly fueled by concern over acid rain and its effects on soils, ecosystems and cation cycling in forests (Pačes, 1983, 1986; Velbel, 1985, 1986; Lindberg *et al.*, 1986; April *et al.*, 1986). By the late 1980s and 1990s, weathering fluxes had been quantified from diverse catchments spanning a wide variety of rock types (Gíslason and Eugster, 1987) and climates (White and Blum, 1995). Thus it became possible to make meaningful site-to-site comparisons and thus gain unprecedented insight into how catchment-scale chemical weathering rates vary with factors such as lithology (Bluth and Kump, 1994), crystallinity (Stefansson and Gíslason, 2001), runoff (Dunne, 1978; Dethier, 1986; Bluth and Kump, 1994), water through-flow in soils (Clow and Drever, 1996), altitude (Drever and Zobrist, 1992), vegetation (Taylor and Velbel, 1991; Drever, 1994; Moulton and Berner, 1998), precipitation (Peters, 1984; White and Blum, 1995), and temperature (White and Blum, 1995; White *et al.*, 1999a). Connections between weathering and climate (Meybeck, 1987) and between chemical and physical erosion (Gaillardet *et al.*, 1999) were also explored during this time using coupled measurements of solute and sediment loading in large rivers. Later, a compilation of solute data from small catchments, including rapidly eroding slopes of the New Zealand Southern Alps (Jacobson and Blum, 2003), was used to explore the effects of climate and tectonics on chemical weathering fluxes from granitic terrain (West *et al.*, 2005).

Though diverse in scope, these and other compilation-based studies of weathering rates have generally shared a foundation in Jenny's (1941) state-factor approach, with study sites chosen to maximize differences in a factor of interest while minimizing variations in potentially confounding factors. The input–output mass balance that lies at the core of many of these compilations is still widely used in studies of catchment-scale weathering fluxes (Bricker *et al.*, 2003; Velbel and Price, 2007). In one of the contributions to this special issue, for example, Price *et al.* (2013) describe how they used the input–output mass-balance approach to quantify calcite weathering rates in the deep CZ.

From laboratory experiments to global geochemical cycles

As field-based studies of solute fluxes proliferated, researchers also increasingly focused on weathering under the more controlled conditions of laboratory experiments. The experimental measurement of rate constants in the kinetics of weathering was a topic of especially vigorous international research from the 1970s to well into the 1990s. The goal was to parameterize weathering rate laws, as cast generically here in terms of the change in concentration (C) of an element or mineral X over time (t). A recent formulation of a simple rate that has been popular in geomorphological literature is shown in Equation (4) (e.g. see Waldbauer and Chamberlain, 2005):

$$\frac{dC}{dt} = -\mathrm{k}AC \tag{4}$$

Here k is the reaction rate constant (in $\mathrm{N\,L^{-2}\,T^{-1}}$) and A is the surface area of the reacting mineral (in $\mathrm{L^2\,N^{-1}}$). Symbols, descriptions, and dimensions of these and other variables and constants used in this review are summarized in Table I.

Data from the laboratory-based studies have been summarized in numerous compendia over the years (Lasaga, 1981; Sverjensky, 1992; Palandri and Kharaka, 2004; Marini, 2006; Bandstra and Brantley, 2008; Bandstra *et al.*, 2008; Oelkers and Schott, 2009; Brantley and Olsen, 2014). The effect of time on weathering rates was an area of particular interest (White and Brantley, 2003). Despite much progress on the subject, researchers still disagree on whether rate constants of dissolution increase, remain constant, or decrease with time (Kump *et al.*, 2000). Even so, time-invariant rate constants are now widely used to predict mineral dissolution rates in reactive transport models (Lichtner, 1988; Steefel *et al.*, 2005; Goddéris *et al.*, 2006; Maher, 2010; Maher, 2011; Moore *et al.*, 2012; Maher and Chamberlain, 2014), under the assumption that the time dependence of dissolution is due to changes in surface area (A) rather than the rate constant (k).

As laboratory experiments proliferated, researchers sought to compare laboratory-based weathering rates with available solute flux data from the field. They found sharp differences that were not easily explained (Pačes, 1983; Velbel, 1985, 1993; Swoboda-Colberg and Drever, 1993). Laboratory-based rates exceeded field-based rates by up to five orders of magnitude.

Table I. Notation.

Symbol	Description	Dimensions
A	Specific surface area of a species of interest	$\mathrm{L^2\,N^{-1}}$
A_f	Area of minerals in contact with through-flowing water	$\mathrm{L^2}$
A_T	Total surface area of the dissolving mineral in a profile	$\mathrm{L^2}$
b	Exponential scaling factor in soil production function	$\mathrm{L^{-1}}$
c	'Hump' parameter in soil production function	$\mathrm{L^{-1}}$
C	Concentration of a mineral in rock	$\mathrm{N\,L^{-3}}$
C_{eq}	Equilibrium concentration of the dissolving mineral X in fluid	$\mathrm{N\,L^{-3}}$
C_X	Molar concentration of species X in rock	$\mathrm{N\,N^{-1}}$
CDF	Chemical depletion fraction of soil	dimensionless
CDF_X	Chemical depletion fraction of element X	dimensionless
D	Sum of chemical and physical erosion rates or regolith production rate	$\mathrm{M\,L^{-2}\,T^{-1}}$
Da	Damköhler number	dimensionless
h	Thickness of soil (mobile regolith)	L
$\mathrm{h_{opt}}$	Optimal soil thickness (corresponding to $\mathrm{P_{max}}$)	L
H	Thickness of regolith (soil plus saprolite)	$\mathrm{M\,L^{-2}}$
$I_{protolith}$	Concentration of insoluble element in protolith	$\mathrm{M\,M^{-1}}$
I_{soil}	Concentration of insoluble element in soil	$\mathrm{M\,M^{-1}}$
k	Reaction rate constant	$\mathrm{N\,L^{-2}\,T^{-1}}$
K	Efficiency of hillslope soil flux	$\mathrm{L^2\,T^{-1}}$
P	Soil production rate	$\mathrm{M\,L^{-2}\,T^{-1}}$
$\mathrm{P_0}$	Soil production rate when $h = 0$	$\mathrm{M\,L^{-2}\,T^{-1}}$
$\mathrm{P_{max}}$	Maximum soil production rate, when $h = \mathrm{h_{opt}}$	$\mathrm{M\,L^{-2}\,T^{-1}}$
$\mathbf{q_{soil}}$	Vector describing soil flux on a hillslope	$\mathrm{L^2\,T^{-1}}$
ρ_{sap}	Density of saprolite	$\mathrm{M\,L^{-3}}$
ρ_{soil}	Density of soil	$\mathrm{M\,L^{-3}}$
T_{reg}	Timescale of regolith weathering	T
T_{adv}	Timescale of advection	T
T_{diss}	Timescale of dissolution	T
τ_X	Mass-transfer coefficient of element X	dimensionless
v	Average flow velocity of fluids in CZ	$\mathrm{L\,T^{-1}}$
V_f	Volume of fluid moving past a mineral surface per time	$\mathrm{L^3}$
W	Weathering flux or chemical erosion rate	$\mathrm{M\,L^{-2}\,T^{-1}}$
W_X	Weathering flux or chemical erosion rate of element X	$\mathrm{M\,L^{-2}\,T^{-1}}$
$X_{protolith}$	Concentration of element X in protolith	$\mathrm{M\,M^{-1}}$
X_{soil}	Concentration of element X in soil	$\mathrm{M\,M^{-1}}$
z	Elevation	L
z_b	Elevation of bedrock–saprolite interface	L
z_c	Elevation below which few fractures in bedrock are open	L
z_{frost}	Elevation of deepest rock damage due to frost cracking	L
z_{sap}	Elevation of saprolite–soil interface	L
z_{surf}	Elevation of topographic surface	L
z_w	Elevation of deepest limits of subsurface weathering	L

A variety of explanations have been proposed over the years to explain the discrepancies (White and Brantley, 2003). For example, it has been noted repeatedly that laboratory-based reactions occur at far-from-equilibrium conditions and that field-based weathering occurs closer to equilibrium. However, Zhu (2005) was perhaps the first to convincingly explain how coupling between mineral reactions might cause slower net reaction rates. Specifically, the coupling between dissolution of primary silicates and the slow rate of precipitation of clays can slow field-based reactions by orders of magnitude relative to laboratory-based rates. A full explanation of the discrepancy between laboratory- and field-based rates also must include arguments about spatial and temporal scaling of local equilibrium (Knapp, 1989) and the production of mineral surface area, as highlighted in this special issue (Bazilevskaya *et al.*, 2013).

The early 1980s saw the first attempts to model effects of weathering on Earth's long-term climatic evolution (Berner *et al.*, 1983). The idea that weathering might be an important regulator of atmospheric carbon dioxide had long since been established (e.g. Urey, 1952). The pressing challenge of the 1980s was to explore the sensitivity of weathering-climate connections at the appropriate scales. The geochemistry of large rivers (Martin and Meybeck, 1979) provided a quantitative basis for global estimates of weathering rates in these models (Berner *et al.*, 1983). Today, models of global geochemical cycles increasingly incorporate descriptions of reaction kinetics (Lerman and Wu, 2008; Roelandt *et al.*, 2010). Yet there are still many unknowns, including the role the deep CZ plays in Earth's carbon cycle. Recent studies of tectonically active settings suggest that weathering in the deep CZ may be particularly important in determining the strength of connections between climate and tectonics (Tipper *et al.*, 2006; Calmels *et al.*, 2011; West, 2012). In this special issue, Rivé *et al.* (2013) documented connections between weathering and volcanically sourced carbon dioxide using carbon isotopes in stream water from the Lesser Antilles. They found that deeply sourced carbon dioxide plays a key role in the rapid rates of silicate weathering that they observed on these islands. To the extent that this is true in volcanic landscapes elsewhere around the world, it implies that the deep CZ may play a significant role in the apportionment of volcanically outgassed carbon dioxide to the atmosphere and other carbon sinks, including dissolved inorganic carbon in groundwater runoff (Rivé *et al.*, 2013).

Solid-phase mass balance studies

Starting in the late 1970s and continuing throughout the 1980s, field-based studies of soils and sedimentary deposits became increasingly quantitative in their use of solid-phase data on soils and mineralogy. New metrics and indices for gauging weathering from soils and regolith were developed (Parker, 1970; Clayton and Arnold, 1972; Nesbitt, 1979; Nesbitt and Young, 1982), as summarized in reviews by Price and Velbel (2003) and White (2008). Perhaps the most significant advance in this area occurred decades earlier, as the mass balance concepts first proposed by Merrill (1897) were developed into quantitative formulae (Marshall and Haseman, 1942; Nikiforoff and Drosdoff, 1943) that were summarized succinctly by Brewer (1964) in his book 'Fabric and Mineral Analysis of Soils.' Equation (5a) shows the formulation later presented by Nesbitt (1979).

$$\%\text{Change} = \left(\frac{X_{soil} I_{protolith}}{X_{protolith} I_{soil}} - 1\right) 100; \tag{5a}$$

$$\tau_X = \frac{X_{soil} I_{protolith}}{X_{protolith} I_{soil}} - 1 \tag{5b}$$

Here, I is the concentration of an insoluble reference element and %Change is the weathering-related mass loss of an element with concentration X, expressed as a percentage of the amount of the element that was present in the protolith. Equation (5b) expresses the loss in fractional rather than percentage terms, as τ_X, the 'mass-transfer coefficient' for element X (Brimhall and Dietrich, 1987). The subscripts *soil* and *protolith* in both equations refer to the CZ materials in which element concentrations are measured. Equation (5a) is essentially identical to the one described in words by Merrill (1897) more than 80 years earlier. To our knowledge, Nesbitt (1979) was the first to employ it in calculating weathering losses using zirconium, an element which is often found in insoluble minerals. Shortly thereafter, April *et al.* (1986) used titanium, another element found in highly insoluble minerals, together with the stable mineral ilmenite, to quantify long-term weathering rates from vertical profiles of base cations and minerals in soils of the Adirondack Mountains in the eastern United States. Starting in 1987, Equation (5b) became the preferred formulation in the literature (Brimhall and Dietrich, 1987). Today, the mass transfer coefficient is often referred to colloquially as 'tau' in studies of soils and chemical weathering.

It was recognized early that tau reflects gains as well as losses from soil profiles for elements that are introduced after bedrock is broken down into regolith (Brimhall and Dietrich, 1987; Chadwick *et al.*, 1990; Brimhall *et al.*, 1991; Merritts *et al.*, 1992). For example, gains in phosphorus might occur, despite the relatively high solubility of its most common bedrock-host-mineral apatite, due to a combination of contributions from the atmosphere and biogeochemical retention in biomass (Merritts *et al.*, 1992). In addition to quantifying mass loss, tau can also be used to quantify volumetric strain (e.g. dilation due to root action and collapse due to mass loss) when both bedrock and regolith density are known (Brimhall *et al.*, 1992). Tau can also be readily applied to studying the deep CZ; if cores from deep boreholes are available it is straightforward to measure down-hole variations in bulk geochemistry and density and thus quantify how tau and strain vary with depth. Though the approach is limited by the ability to characterize protolith (which, by definition, is altered in the regolith), it was popularized by Art White and colleagues to study deep CZ weathering at numerous locales (White, 1995, 2002; White *et al.*, 1996, 1998, 2001) and has now been used worldwide by geomorphologists in areas such as south-eastern Australia (Burke *et al.*, 2009), the coast ranges of California (Burke *et al.*, 2007) and Oregon (Anderson *et al.*, 2002), and also at two study sites featured in contributions to this special issue (Brantley *et al.*, 2013; Bazilevskaya *et al.*, 2013).

The derivation of tau is based on the assumption that parent material is lost solely by chemical weathering, and does not include terms for mass losses due to physical erosion of fine colloidal material (e.g. Bern *et al.*, 2011, 2015) and larger fragments (Riebe *et al.*, 2001a). However, as shown next, an expression that is mathematically identical to tau, except in algebraic sign, emerges from the input–output mass balance for eroding soils, as first demonstrated by Stallard (1985). He wrote an expression similar to Equation (6), which accounts for both chemical and physical erosion in a steady-state weathering profile (i.e. where regolith thickness and geochemistry do not change over time).

$$W_X = D X_{protolith} \left(1 - \frac{X_{soil} I_{protolith}}{X_{protolith} I_{soil}}\right) \tag{6}$$

Here W_X is the chemical weathering flux of element X, and D is the downward propagation rate of the weathering front at the

bedrock-saprolite interface, also known as the 'weathering advance' or 'regolith production' rate. Both W_X and D are expressed in dimensions $\mathrm{M\,L^{-2}\,T^{-1}}$ in this formulation. Under the steady-state assumption of Equation (6), D is also equal to the overall (i.e. chemical plus physical) erosion rate of the landscape.

Stallard's (1985) mass-balance formulation was an advance over the formulation for physically stable (non-eroding) soils. It made the approach explicitly applicable to a wider range of settings, including soils undergoing considerable physical erosion as they are physically broken down and chemically weathered on slopes (White *et al.*, 1998). Moreover, Equation (6) provides a way to tease the chemical and physical processes apart. For example, it can be rearranged to solve for the 'chemical depletion fraction' of element X, denoted by CDF_X and defined as the fraction of the overall erosion rate of the element that is accounted for by chemical losses (Riebe *et al.*, 2003).

$$\mathrm{CDF}_X = \frac{W_X}{DX_{protolith}} = \left(1 - \frac{X_{soil} I_{protolith}}{X_{protolith} I_{soil}}\right) \tag{7}$$

Thus even when the chemical erosion rate is not measured in absolute terms, it can be expressed in relative terms as a fraction of the overall throughput of material in the weathering engine. The only measurements that are needed, according to Equation (7), are bulk and trace element concentrations in both soil and bedrock.

Steady-state mass-balance formulations can also be written for the regolith as a whole (i.e. integrated over all of the constituent elements) as shown in Equations (8) and (9) (Riebe *et al.*, 2001b).

$$W = D\left(1 - \frac{I_{protolith}}{I_{soil}}\right) \tag{8}$$

$$\mathrm{CDF} = \frac{W}{D} = \left(1 - \frac{I_{protolith}}{I_{soil}}\right) \tag{9}$$

Here, W, D and CDF respectively refer to the chemical erosion rate, the overall (physical plus chemical) erosion rate and the chemical depletion fraction for the regolith as a whole. Each of these values could vary across the landscape. Furthermore, both the protolith and soil can harbor substantial lateral and vertical spatial variability in both X and I. When they do, it may help to collect and analyze many samples of soil and protolith and use average values of element concentrations in Equations (6)–(9) for spatially averaged values of W and CDF. However, this requires the generally untested assumption that simple averaging can appropriately integrate the potentially complicated mosaic of weathering across a landscape.

In this steady-state formulation of Equation (7), CDF_X is equivalent except in algebraic sign to the expression for tau in Equation (5b). Despite the equivalence in these mathematical formulations, CDF and tau are different in at least one way; whereas CDF_X is by definition the ratio of chemical to total (i.e. chemical plus physical) erosion, tau is the mass transfer coefficient, derived to reflect the chemical loss or gain of mass relative to the original mass present in the protolith. The derivation of Equation (5b) assumes that the entire allotment of the insoluble element in the protolith is still present in the weathered sample of interest. This is not the case for samples of eroding soil at the surface, because some of the insoluble elements are lost from the top of the regolith profile by physical erosion. The seemingly contradictory definitions of two indices that can be calculated using essentially the same mathematical expression highlights the crucial importance of understanding the context of the samples that have been collected. In a strict sense, CDF_X may be the more useful concept for interpreting weathering from samples of eroded soil at the surface, whereas tau may be the more useful concept for understanding weathering both at the top of non-eroding profiles and below the physically mixed soil in any profile (eroding or non-eroding). Thus whereas CDF_X can generally be used as a single value to denote depletion of an entire soil, tau is well suited to quantifying variations in depletion as a function of depth. For additional discussion on connections between CDF_X and tau we point readers to Brantley and Lebedeva (2011).

Stallard's (1985) derivation of Equation (6) explicitly accounts for gradients in regolith geochemistry. In a series of studies published in 1998, Art White and colleagues employed Stallard's framework to study a thick weathering profile on a ridgetop in the Rio Icacos watershed, Puerto Rico. They used lysimeters to sample gradients in pore-fluid composition (Stonestrom *et al.*, 1998) and an auger to sample across gradients in soil and saprolite bulk geochemistry (White *et al.*, 1998) and mineralogy (Murphy *et al.*, 1998). Weathering rates calculated from the profile were the fastest ever reported in the literature for granitic terrain and agreed remarkably well with estimates based on catchment-wide solute fluxes from a nearby stream (McDowell and Asbury, 1994). The Puerto Rico field area soon became a mecca for the study of intense weathering (Riebe *et al.*, 2003; Turner *et al.*, 2003; Kurtz *et al.*, 2011) and other CZ processes (Richardson *et al.*, 2000; Merriam *et al.*, 2002) in the humid tropics, setting the stage for the Luquillo CZO, established in 2009, which included a neighboring watershed that had already been studied for many years by ecologists (Scatena, 1989). A number of studies of the deep CZ at the Luquillo CZO have followed (Buss *et al.*, 2008, 2010; Ferrier *et al.*, 2010; Fletcher and Brantley, 2010; Chabaux *et al.*, 2013; Dosseto *et al.*, 2012, 2014), including one described in a contribution to this special issue (Buss *et al.*, 2013).

Millennial-average rates of physical and chemical erosion

White and colleagues successfully used Equation (6) in Puerto Rico in 1998. However, in 1985, when it first appeared in a book chapter penned by Stallard, there was no widely applicable method for measuring D over the timescales of soil formation. So there was no ready way to use Equation (6) to study how chemical erosion rates vary across landscapes. This limitation soon vanished with the widespread application of cosmogenic nuclides in surface processes research, beginning in the mid-1980s with a series of publications on accelerator mass spectrometry (AMS) and the measurement of cosmogenic helium-3 (^{3}He), beryllium-10 (^{10}Be), aluminum-26 (^{26}Al), and chlorine-36 (^{36}Cl) in terrestrial rocks and soils (Pavich *et al.*, 1985; Kurz, 1986; Nishiizumi *et al.*, 1986; Phillips *et al.*, 1986; Elmore and Phillips, 1987). Cosmogenic nuclides average erosion rates over the time required to erode 1–2 m of soil (depending on density). This makes them nearly ideal for studying processes of soil formation, weathering, and erosion in landscapes (Granger and Riebe, 2014; Dixon and Riebe, 2014). For example, by 1996, it had been shown that the concentrations of cosmogenic ^{10}Be and ^{26}Al in quartz from sediment collected from catchment streams could be used to infer spatially averaged erosion rates for the entire sediment contributing area (Brown *et al.*, 1995; Bierman and Steig, 1996; Granger *et al.*, 1996). The method is complicated by a number

of factors, including spatial variations in the sizes of sediment produced by weathering on slopes (Lukens *et al.*, 2016) and preferential chemical erosion of relatively soluble minerals, which biases interpretation of cosmogenic nuclides from quartz in soils and sediment (Small *et al.*, 1999). However, methods have now been developed to account for variations in sediment size (Riebe *et al.*, 2015) and the chemical erosion bias (Riebe *et al.*, 2001a). One of the contributions to this special issue (Riebe and Granger, 2013) provides a way to realistically account for deep weathering as well as weathering that occurs near the surface in soil.

Cosmogenic nuclides have made it possible to quantify long-term rates of overall (chemical plus physical) erosion (i.e. D) and thus use Equation (6) to infer long-term chemical erosion rates across a wide range of actively eroding landscapes (Riebe *et al.*, 2001b). In this approach, chemical and physical components of erosion are measured together over comparable timescales, making the measurements applicable to quantifying how chemical and physical erosion interrelate (e.g. Riebe *et al.*, 2001b; Ferrier *et al.*, 2016). Equation (6) was eventually adapted to quantify mineral-specific chemical erosion rates (White 2002; Ferrier *et al.*, 2010), to gauge the relative importance of saprolite weathering (White *et al.*, 1998; Dixon *et al.*, 2009), and to quantify the fractional contributions of airborne dust to the mass balance of catchment soils (Ferrier *et al.*, 2011). Compilations of these types of measurements across gradients in climate and tectonics have greatly enhanced understanding of factors that regulate chemical erosion and regolith development across landscapes (Riebe *et al.*, 2004; von Blanckenburg, 2005; Lebedeva *et al.*, 2010; Rasmussen *et al.*, 2011b; Dixon and von Blanckenburg, 2012; Chadwick *et al.*, 2013; Larsen *et al.*, 2014).

Millennial-average rates of soil production

Cosmogenic nuclides have also been used to quantify soil production rates from *in situ* produced nuclides in samples of saprolite collected from the base of soils (Heimsath *et al.*, 1997) and from meteoric nuclides in samples of soil collected along slopes (Monaghan *et al.*, 1992; Monaghan and Elmore, 1994). In these studies, 'soil' has usually been defined to mean 'mobile soil', or the part of the regolith that moves downslope on a hillside. Thus cosmogenic nuclides have enabled the first quantitative tests of Gilbert's (1877) hypothesis about the soil production function (Humphreys and Wilkinson, 2007). The hypothesis can be expressed quantitatively, and thus in a readily testable form, using a simple, three-parameter formula (after Cox, 1980).

$$P = P_0 e^{-bh}(1 + ch) \tag{10}$$

Here P is the soil production rate (in $M\,L^{-2}\,T^{-1}$), h is soil thickness (in L), and P_0 is the production rate under zero soil thickness. The parameter b (L^{-1}) is a scaling factor for the decrease in production rate with increasing h, and c (in L^{-1}) determines the thickness at which soil production is maximized for a given value of b if the relationship is humped. For $c = 0$, the hump vanishes and Equation (10) reduces to a negative exponential, with maximum production rate (P_{max}) equal to P_0 at $h = 0$. Otherwise, P_{max} occurs where $dP/dh = 0$, at an optimal soil thickness (h_{opt}) that can be calculated from Equation (11).

$$h_{opt} = \frac{c - b}{cb} \tag{11}$$

For $c > 0$, P_{max} can be calculated using Equation (12).

$$P_{max} = \frac{P_0 c}{b} e^{(b-c)/c} \tag{12}$$

Hence, Equation (10) flexibly captures both the humped soil-production function proposed by Gilbert and the alternate hypothesis that soil production rates decrease monotonically as an exponential function of increasing soil thickness (Cox, 1980). Both humped and exponential versions of Equation (10) are plotted in Figure 3 for illustration.

Cosmogenic nuclide-based studies of soil production functions have now spanned the globe (Dixon and Riebe, 2014). Although many landscapes have been shown to harbor an exponential decline in soil production rate with increasing thickness (Heimsath *et al.*, 1999, 2000), both humped (Riggins *et al.*, 2011) and relatively flat (Wilkinson *et al.*, 2005; Dixon *et al.*, 2009) functions have also been observed. Exponential declines in soil production rates have now also been documented using soil production rates measured from uranium isotope disequilibrium measurements (e.g. Ma *et al.*, 2010). We point readers to Minasny *et al.* (2008) for a recent review of quantitative studies of soils and to Heimsath *et al.* (2012) for a meta-analysis of linkages between soil production and catchment-wide erosion.

Regolith fluxes across slopes

In addition to fueling important research on soil production, erosion and weathering, cosmogenic nuclides have enabled major advances in understanding the physical flux of regolith across slopes. The application builds on the first geomorphic

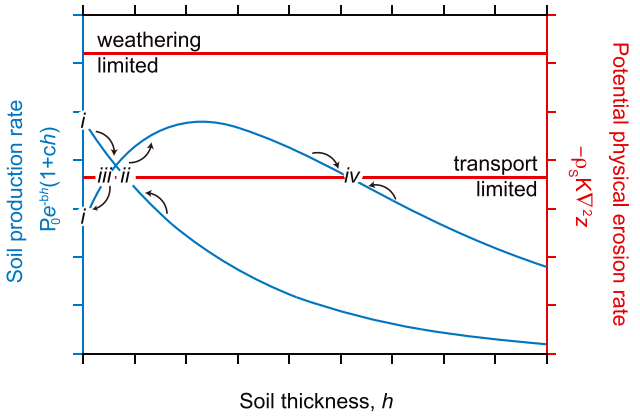

Figure 3. Relationship between soil production rate (blue lines, left axis) and soil thickness, including two differing rates of potential physical erosion (red lines, right axis) which can be conceptualized as being either weathering- or transport-limited as indicated. The humped and monotonic soil production functions have the same parameters b and P_{max} (see Equations (10)–(12)). Because the upper rate of potential physical erosion (upper red line) is greater than P_{max}, erosion is 'weathering limited'; it cannot exceed a rate of P_0 (which is lower for the humped function, as indicated by positions of numerals *i* on the plot). In this case, soils are stripped away because soil production is unable to keep pace with erosion. In contrast, multiple stable soil thicknesses are possible in the transport-limited case, where potential erosion (lower red line) is less than P_{max}. In the monotonic function, soils tend toward a single stable thickness at which soil production rate equals the potential erosion rate (case ii). In the humped function, the soil production rate will balance the potential erosion rate at one of two soil thicknesses (case iii or iv). Case iii is unstable: if soils become thinner, thickness again stabilizes at a thickness of zero with $P = P_0$ (case i). If soils instead get thicker, then soil thickness stabilizes at the higher of the two values (case iv), which is then stable against perturbations. Adapted from Stallard (1985). [Colour figure can be viewed at wileyonlinelibrary.com]

transport law (Dietrich *et al.*, 2003) introduced by Gilbert and Davis a century ago. According to the hypothesis behind that transport law, the sediment flux should increase systematically with hillslope gradient. This hypothesis was re-envisioned more quantitatively in the early 1960s by Culling (1960, 1963), in the first efforts to model hillslope evolution using a geomorphic transport law. As a working hypothesis, Culling (1960) expressed the volumetric regolith flux per unit contour width (in $L^2\,T^{-1}$) as a vector ($\mathbf{q_{soil}}$) that increases linearly with the gradient in surface topography (∇z).

$$\boldsymbol{q}_{soil} = -K\nabla z \tag{13}$$

Here K is the efficiency of hillslope sediment flux (in $L^2\,T^{-1}$).

The relationship in Equation (13) can be readily applied to landscape evolution modeling by coupling it with a mass balance of regolith on a slope (Figure 4). Equation (14) describes the continuity of mass for mobile regolith under the assumption that fluxes due to dissolution are negligible (Culling, 1960; Dietrich *et al.*, 2003).

$$\rho_{sap}\frac{dz_{sap}}{dt} = -\rho_{soil}\nabla\cdot\boldsymbol{q}_{soil} - \rho_{soil}\frac{dh}{dt} \tag{14}$$

Here, ρ is density, the subscripts *soil* and *sap* refer to the soil (i.e. the mobile regolith) and the underlying substrate from which it was generated (e.g. saprolite, saprock or bedrock), respectively. The product of ρ_{soil} and dh/dt, the rate of change in soil thickness, is a change-in-storage term. Note that the product of saprolite density, ρ_{sap}. and the lowering rate of the soil–bedrock interface, $-dz_{sap}/dt$, is equivalent to P, the soil production rate, which we expressed as an empirical function of depth in Equation (10).

Combining Equations (13) and (14) and assuming soil thickness is steady (i.e. such that $dh/dt = 0$ in Equation (14)) leads to Equation (15) (see also Figure 4), which expresses the soil production rate as a function of hillslope curvature, $\nabla^2 z$ (Dietrich *et al.*, 1995).

$$P = -\rho_{sap}\frac{dz_{sap}}{dt} = -\rho_{soil}K\nabla^2 z \tag{15}$$

On convex slopes, $\nabla^2 z < 0$, such that $P > 0$. As Culling (1960) pointed out, K is analogous to the diffusivity term in heat transfer across temperature gradients. Thus, Equations (13) and (15) imply that transport processes on slopes can be broadly thought of as diffusive; material generally spreads from areas with high hillslope gradients to areas of low hillslope gradients, thus smoothing over any high and low points along the slope. Lebedeva and Brantley (2013) modified Equation (15) to include a term for chemical losses and solved it for a two-dimensional (2D) hillslope using a reactive transport algorithm.

Other formulations for $\mathbf{q_{soil}}$ have been proposed over the years, recognizing the potential importance of both depth-dependent and non-linear slope-dependent transport in soil-mantled landscapes that lack the characteristic convex topography of linear diffusion. Equation (14) implies that $\mathbf{q_{soil}}$ depends only on local hillslope gradient and not on the thickness of the mobile soil layer. Recently, a theoretical basis for soil-depth dependence has been explored (Heimsath *et al.*, 2005; Furbish *et al.*, 2009) and used to explain sediment transport across slopes with soil thicknesses that vary periodically downslope (Johnstone and Hilley, 2015). In rapidly uplifting landscapes, a sharp downslope increase in sediment transport as slopes steepen past a critical slope (Anderson and Humphrey, 1989) may be needed to help explain the downslope transition from convex to planar slopes often observed in mountainous terrain (Roering *et al.*, 1999). Even when such conditions exist, Equations (13)–(15) may reflect a reasonable approximation of sediment transport across convex hilltops (Roering *et al.*, 1999; Hurst *et al.*, 2012). When this is true, K can be inferred from cosmogenic nuclides via two approaches: using Equation (13) with estimates of $\mathbf{q_{soil}}$ from atmospherically deposited ('meteoric') ^{10}Be in soils (Monaghan *et al.*, 1992 and McKean *et al.*, 1993; Graly *et al.*, 2010; Willenbring and von Blanckenburg, 2010); and using Equation (15) with estimates of P from *in situ* produced cosmogenic nuclides in the top of saprolite (following Dietrich *et al.*, 1995 and Heimsath *et al.*, 1997). Once K is known, it may be possible to couple it with estimates of hilltop curvature (e.g. from LiDAR [light detection and ranging]) to infer the spatial distribution of soil production and erosion across landscapes (Hurst *et al.*, 2012; Hurst *et al.*, 2013).

In a relatively recent advance, variations in chemical erosion fluxes have been quantified along hillslopes by combining geochemical mass-balance measurements (e.g. Equations (6)–(9)) with cosmogenic nuclide estimates of soil production rates

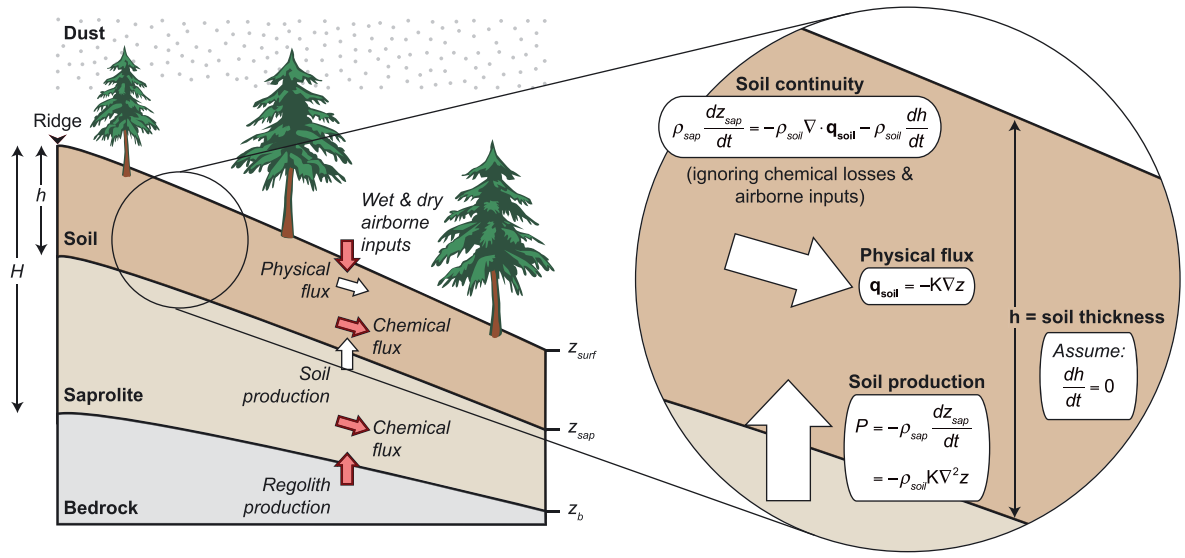

Figure 4. Schematic showing mass fluxes on a slope. Conversion of rock to saprolite is the regolith production rate. Regolith is then lost by mineral weathering in the soil and saprolite and by physical erosion of soil. Exploded view shows the mass balance of Equations (13) to (15), which focuses on just the production and physical erosion of soil, ignoring chemical fluxes in the soil and saprolite, additions of airborne material from above, and production of regolith at depth (depicted with red arrows at left). [Colour figure can be viewed at wileyonlinelibrary.com]

(Green *et al.*, 2006; Yoo *et al.*, 2007, 2009). The approach involves a more expansive and ultimately more complete continuity formulation than the one expressed in Equation (14) (see for example Minasny and McBratney, 2001; Green *et al.*, 2006; Yoo *et al.*, 2007, 2009; Jin *et al.*, 2010). It also requires more measurements to quantify how the bulk geochemistry of soil and saprolite change downslope from drainage divide to the toe of the slope where soil enters the channel network.

Regolith production rates: a new frontier

Many of the CZ fluxes illustrated in Figure 4 can now be measured using various applications of cosmogenic nuclides in soils, saprolite and sediment. However, cosmogenic nuclides are not generated quickly enough in deep regolith to reliably quantify regolith production rates in many landscapes. If a method could be developed for measuring how regolith production rates vary across landscapes, it would open up a new class of studies of connections between weathering in the deep CZ and the topography, climate and biota that drive surface processes. One solution may lie in the measurements of weathering timescales from uranium-series disequilibrium dating (Dosseto *et al.*, 2006, 2008, 2014; Chabaux *et al.*, 2008; Ma *et al.*, 2010, 2013). In the Shale Hills CZO for example, analysis of regolith production rates from uranium-series measurements (Ma *et al.*, 2013) are in good agreement with erosion rates implied by the buildup of meteoric ^{10}Be in soils (West *et al.*, 2013). Thus, the coupled application of uranium-series dating and cosmogenic nuclides to quantifying rates of regolith production and erosion appears to be an important frontier in deep CZ research.

Speed limits on erosion and weathering

Our review shows that, for decades, measurements of rates of physical erosion, weathering, and the production of both regolith and soil have been central in advances in geomorphology, geochemistry and pedology. The database of these kinds of measurements has grown to span the globe. This has revealed great complexity in how erosion and weathering interrelate and how they are regulated by climate, biology, lithology and tectonics (von Blanckenburg, 2005; Moon *et al.*, 2011; Portenga and Bierman, 2011; Rasmussen *et al.*, 2011b; Dixon and von Blanckenburg, 2012; Chadwick *et al.*, 2013; Hahm *et al.*, 2014).

To help understand the complexity, geomorphologists and geochemists alike have developed rate-limiting frameworks for interpreting surface processes in simplified terms (Carson and Kirkby, 1972; Stallard and Edmond, 1983; White *et al.*, 2001; Riebe *et al.*, 2004; West *et al.*, 2005; Ferrier and Kirchner, 2008; Gabet and Mudd, 2009; Hilley *et al.*, 2010; Lebedeva *et al.*, 2010). Although applications of these frameworks have been useful and enlightening, confusion has arisen over their nomenclature and use as scientists have reached across disciplines and spatial scales to investigate the CZ (Brantley *et al.*, 2014). In fact, our attempts to reduce the confusion, presented next, differ in many details from a similar-themed discussion in a recent review of weathering fronts and subsurface reactants (Brantley *et al.*, 2014) led by one of us. In this revision of that previous discussion, we sometimes define terms differently, but only where we have sought to retain older definitions.

Here we focus on the three main frameworks that are relevant to the deep CZ: (i) solute-transport versus interface limitations used by geochemists to explain mineral weathering rates at the grain scale; (ii) weathering versus transport limitations used by geomorphologists to explain physical erosion rates of mobile regolith at pedon to catchment scales; (iii) supply versus kinetic limitations used by geomorphologists and geochemists to explain chemical erosion rates measured at the pedon to catchment scales. Our goal is to compare and clarify these frameworks and show how they can be combined together to cross disciplines for a richer understanding of CZ processes (Figure 5).

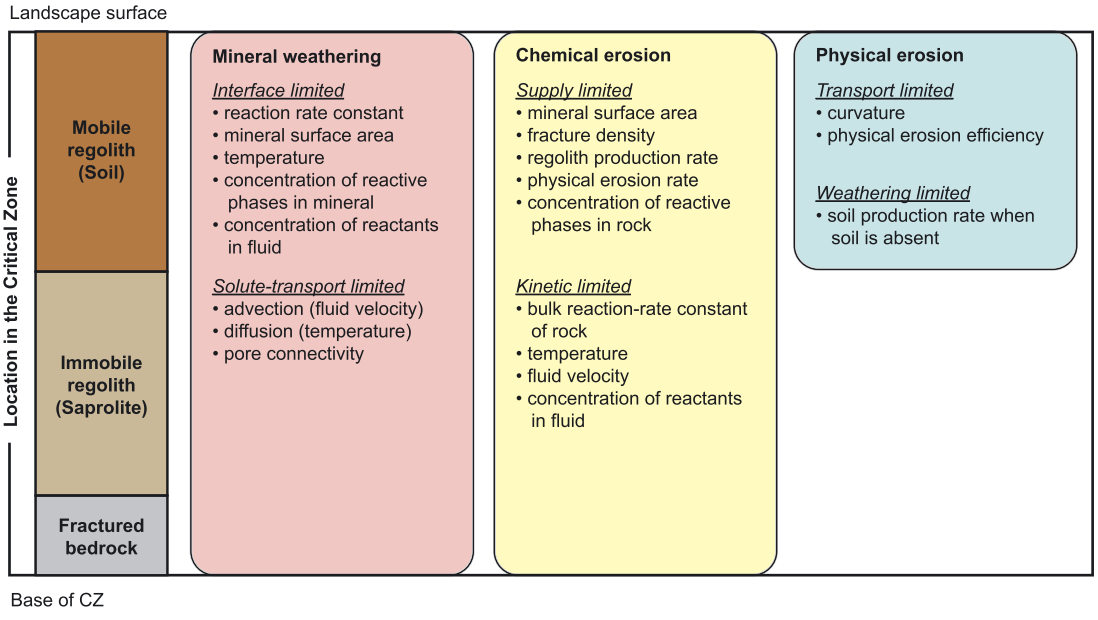

Figure 5. Locations within the critical zone (CZ) and relevant parameters of frameworks for evaluating limitations on rates of mineral weathering, chemical erosion, and physical erosion. Left axis defines position in CZ where the rate-limiting framework is typically applied in the sense originally proposed in the literature. The framework for evaluating mineral weathering can be applied to any position in the CZ but has generally been invoked at the scale of individual grains and pedons. In contrast, the framework for evaluating chemical erosion fluxes has been applied over control volumes of considerable scale (i.e. pedons or catchments), and generally applies across the entire thickness of the CZ (from its base to the landscape surface). Meanwhile the framework for evaluating physical erosion was developed to interpret processes that produce or move mobile regolith or soil (generally just the upper part of the CZ) and applies to pedons and catchments. [Colour figure can be viewed at wileyonlinelibrary.com]

Solute-transport and interface limitations on mineral weathering

Discussion of solute transport- and interface-limited mineral weathering has been a staple in the low-temperature geochemistry literature for nearly forty years (e.g. Berner, 1978; Brantley *et al.*, 1986; White *et al.*, 2001; West *et al.*, 2005; Maher, 2010, 2011; Maher and Chamberlain, 2014). In the solute-transport-limited regime, minerals are in thermodynamic equilibrium with surrounding pore fluids (e.g. below the base of the CZ), and mineral weathering is limited by solute transport to or away from reacting interfaces (Berner 1978). In the interface-limited regime, minerals are out of equilibrium with surrounding fluids and weathering is limited by reaction rates.

Solute transport limitations on mineral weathering should be important at the deepest depths in the CZ, where the ratio of water to rock is low, advection rates are relatively slow, and most solute transport occurs by diffusion. As fracture density increases closer to the surface, the volume of fluids interacting with a given mass of rock increases. As a result, the fraction of material in which solute transport is restricted to diffusion becomes smaller. Eventually, the volume of fluid relative to reactive mineral surface area increases to the point that mineral weathering becomes increasingly limited by reaction rates, which depend on mineral surface area and reaction rate constants (e.g. see Equation (1)). Under this condition, which has been referred to as interface-limited weathering (Brantley *et al.*, 1986), temperature, mineral composition, and reactant concentrations (e.g. O_2 and CO_2) in pore fluids play crucial roles in setting reaction rates. However, even at the shallowest depths of the CZ, diffusion may dominate solute transport in the cores of individual mineral grains, rock fragments, and in blocks between fractures. Thus minerals at these shallower depths can remain far from equilibrium with surrounding pore fluids. However, the volume of such diffusion-only domains is a smaller fraction of the total rock material near Earth's surface than it is at depth.

The dimensionless Damköhler number, *Da*, provides a metric for comparing rates of fluid advection to rates of weathering reactions in regolith profiles. Thus it provides a basis for evaluating whether minerals in the system are weathering in the interface- or solute-transport-limited regime, as shown in Equation (16) (after Salehikhoo *et al.*, 2013).

$$\mathrm{Da} = \frac{T_{adv}}{T_{diss}} = \frac{HWA_T}{vV_pC_{eq}} \tag{16}$$

Here, T_{adv} is the characteristic timescale for advection, equal to the residence time of fluid in the profile; it can be estimated by dividing the overall thickness of the profile, H (in L), by the average flow velocity, v (in LT^{-1}). Meanwhile, the characteristic timescale for dissolution, T_{diss}, which is the time required to reach equilibrium, can be calculated from the rest of the terms: V_p is the total pore volume of the column (in L^3); C_{eq} is the equilibrium concentration of the dissolving mineral in solution (in NL^{-3}); W is the profile-scale dissolution rate ($\mathrm{NL}^{-2}\mathrm{T}^{-1}$); and A_T is the total surface area of dissolving mineral in the profile (in L^2). When the Damköhler number is low ($\mathrm{Da} << 1$), the system is far from equilibrium, consistent with interface-limited mineral weathering. Conversely, when the Damköhler number is high ($\mathrm{Da} >> 1$), the system is close to equilibrium, consistent with solute-transport limited mineral weathering.

Transport and weathering limitations on physical erosion

For more than a century, geomorphologists have been writing about transport and weathering-limited physical erosion. Gilbert (1877) was perhaps the first to discuss this endmember framework in 'Land Sculpture', a chapter in his 1877 Henry Mountains report:

> Over nearly the whole of the earth's surface there is a soil, and wherever this exists we know that the conditions are more favorable to weathering than to transportation. Hence it is true in general that the conditions which limit transportation are those which limit the general degradation of the surface.

This quote neatly encapsulates the concept of transport-limited physical erosion in landscapes.

Likewise, Gilbert's (1877) description of a humped soil production function, quoted earlier, succinctly outlines the concept of weathering limitations on physical erosion: When transport is fast enough to remove a soil completely, both the breakdown and removal of bedrock are 'checked' (Gilbert, 1877). Under this condition, the erosion rate of soil is ultimately limited by the breakdown rate of the underlying saprolite and rock. Although the concepts of transport and weathering limitations in landscapes did not receive much attention at first, they were revived by Carson and Kirkby (1972) and have been frequently employed by geomorphologists ever since.

We stress that the usage of 'weathering' in the term 'weathering limitation' refers specifically to the production of mobile regolith, contrary to its usage both elsewhere in this manuscript and in the parlance of geochemists. In this context, which is familiar to geomorphologists but unorthodox to geochemists, 'weathering' does not apply strictly to dissolution, but rather includes all the biotic and abiotic processes that disrupt intact regolith or weathered bedrock, generate mobile fragments of rock or saprolite, and entrain them into the soil. In effect, the term is a proxy for what we have referred to as 'soil production' elsewhere this manuscript. Thus by itself, the nomenclature in the geomorphologist's rate-limiting framework has potential to introduce considerable semantic confusion among scientists from different disciplines and is likely one of the reasons why discrepancies have arisen in the way it has been invoked over the years. Here we retain the original terminology as closely as possible to try to bridge the gap between the original and later work.

The two endmember limitations on physical erosion are illustrated conceptually in Figure 6 (a-b). This figure also illustrates how one could quantitatively distinguish landscapes according to the endmembers. If the production of mobile soil from saprolite (or bedrock on profiles without saprolite) outpaces the potential erosion, which is expressed as $-\rho_{\mathrm{soil}}\mathrm{K}\nabla^2 z$ in Equation (15) (see also Figure 3), then physical erosion will be 'transport limited' (Figure 6a). In transport-limited physical erosion, an increase in K or $\nabla^2 z$ will increase the physical erosion rate (Figure 3) up to the point that the production of mobile regolith from saprolite or bedrock can no longer keep pace with the increase in transport rate (Figure 6a). If the potential physical erosion rate increases enough that it exceeds P_{max} (Figure 3), the maximum soil production rate, then physical erosion becomes weathering limited (Figure 6b). In that case, the overall rate of physical erosion would be limited by P_0, the rate of soil production from exposed bedrock (Figure 3). An analogous situation arises in fluvial systems when transport exceeds the detachment of bedrock from the riverbed (e.g. Howard, 1994).

Supply and kinetic limitations on chemical erosion

Over the last two decades, since the advent of new tools for quantifying rates of physical and chemical erosion at catchment scales, a relatively new framework of rate limitations has been increasingly invoked to interpret rates of chemical

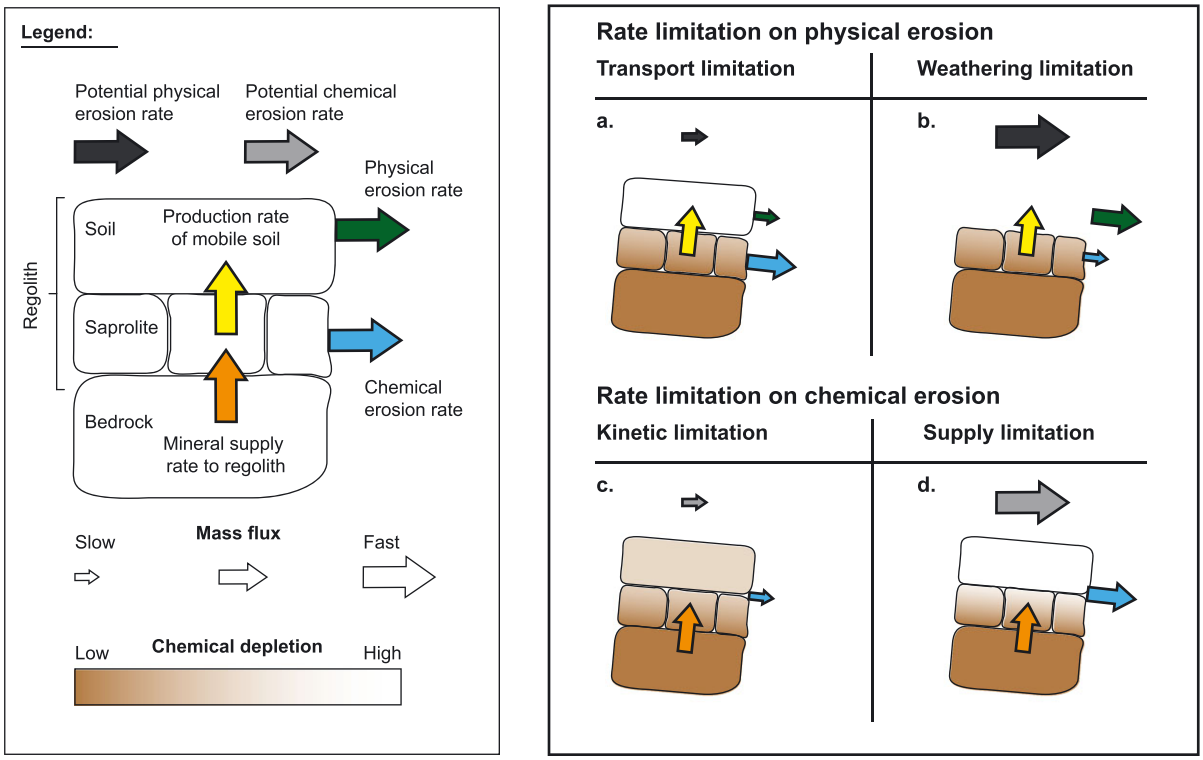

Figure 6. Rate limitations on physical and chemical erosion fluxes from regolith. Here, the framework for interpreting chemical erosion fluxes is distinguished from the framework for interpreting mineral weathering by the difference in scale over which the weathering rate is observed and modeled. Chemical erosion fluxes are measured over pedon and catchment scales while mineral weathering is conceptualized and measured over grain to pedon scales. (a) When the capacity for production of mobile soil from saprolite (yellow arrow) exceeds the potential physical transport from the slope (black arrow), physical erosion (green arrow) is transport limited and soils are typically thick and intensely depleted in mobile elements (shading). (b) Conversely, when the production of mobile soil is slow compared to potential physical transport, physical erosion is weathering limited, and soils are thin or absent. A separate set of rate limitations has been used to interpret chemical erosion fluxes from pedons and catchments (c–d). When the potential for chemical erosion (gray arrow) is low compared to the supply of fresh minerals to the regolith (orange arrow), chemical erosion (blue arrow) is kinetic limited, and the extent of depletion of elements from regolith decreases with increasing supply rates (c). When chemical erosion potential is high relative to fresh mineral supply rates, chemical erosion is supply limited, and chemical depletion is uniform across a range of mineral supply rates (d). [Colour figure can be viewed at wileyonlinelibrary.com]

erosion from mountain soils and catchments. The two endmembers are kinetic-limited and supply-limited chemical erosion (Riebe *et al.*, 2004; Gabet, 2007; Hren *et al.*, 2007; Ferrier and Kirchner, 2008; Hilley and Porder, 2008; Dixon *et al.*, 2009; Gabet and Mudd, 2009; Hilley *et al.*, 2010; Rasmussen *et al.*, 2011b; Lebedeva *et al.*, 2010; Lebedeva and Brantley, 2013; Ferrier *et al.*, 2016). In distinguishing this geochemical framework from the transport- and weathering-limited framework of geomorphologists, it is vital to first distinguish the supply of fresh minerals to the regolith, where the minerals lose mass due to chemical weathering (Figures 6c and 6d), from the supply of saprolite to mobile soil, where minerals are swept away by physical erosion (Figures 6a and 6b).

In kinetic-limited chemical erosion (Figure 6c), regolith should weather to a degree that depends solely on kinetic factors such as temperature, fluid chemistry and throughflow rate, and the bulk reaction rate constant (e.g. Hilley *et al.*, 2010; Lebedeva *et al.*, 2010; Ferrier *et al.*, 2016). Under this condition, chemical erosion fluxes should be insensitive to differences in the supply rate of reactive minerals to the CZ (i.e. $DX_{protolith}$ in Equation (6)) across a suite of sites with a range in mineral supply rates (Figure 6c). If climate, lithology and other factors that regulate mineral weathering are roughly uniform, chemical erosion fluxes should be roughly the same in kinetic-limited erosion, even when there are marked differences in mineral supply rates (Riebe *et al.*, 2004; Ferrier and Kirchner, 2008). Regolith will therefore be less depleted at sites with higher supply rates, because they have lower mineral residence times (for the same soil thickness), leading to fresher regolith at the surface (i.e. with a lower CDF in steady state). The overall chemical erosion flux from the profile can thereby remain roughly uniform across a range of supply rates; lower depletion is compensated by the faster throughput of material that results from faster regolith production at depth and faster erosion at the surface.

At the other end of the spectrum, in supply-limited chemical erosion, weathering reactions are fast enough that all of the reactive minerals in the soil are chemically eroded away (Hilley *et al.*, 2010; Lebedeva *et al.*, 2010; Rasmussen *et al.*, 2011b; Ferrier *et al.*, 2016), leading to 'completely developed' weathering profiles in the parlance of some geochemists (e.g. Lebedeva *et al.*, 2010). Chemical weathering always exhausts the supply of minerals under this condition such that chemical depletion within regolith is the same (i.e. with uniform CDF), irrespective of any differences in supply rate to the regolith column. Under this condition, an increase in the supply rate of reactive phases will cause a proportional increase the total chemical erosion rate but no change in CDF (Figure 6d). This is because material in the profile is being fully depleted (to the same degree) even though it is being pumped through the system more quickly under the higher supply rate.

Kinetic-limited chemical erosion can be distinguished from supply-limited chemical erosion using bulk geochemical measurements of CDF and cosmogenic nuclide-based estimates erosion rates (Ferrier *et al.*, 2016). Across a sufficiently large range in erosion rates, the slope of the power-law relationship

between CDF and the erosion rate (which is a proxy for mineral supply rates in steady state) represents the sensitivity of chemical depletion to variations in mineral supply rates. If the slope of the relationship is zero, it implies that chemical erosion is supply limited; increases in supply rates lead to no change in CDF and thus a proportional increase in chemical erosion rates. Meanwhile, a slope of −1 implies that chemical erosion is kinetic limited; an increase in supply rates leads to a proportional decrease in CDF and thus no change in chemical erosion rates, implying that changes in kinetic factors – not supply rates – are needed to induce changes in chemical erosion rates. A recent meta-analysis showed that few available datasets of CDFs and erosion rates have sufficient statistical power to distinguish between the end-member scenarios, and among those that do, supply-limited conditions are more common (Ferrier *et al.*, 2016).

Linking the historical frameworks

The three rate-limiting frameworks outlined above have several key differences and a conflicting nomenclature that make it challenging to cogently link them together. One way to think about the differences among the frameworks is to consider the scales and locations over which they are relevant within the regolith column (Figure 7). By definition, soil production occurs in the upper part of saprolite (or bedrock, if saprolite is absent) and physical erosion occurs in the upper, mobile part of the regolith column, placing the geomorphic framework (i.e. transport and weathering limited physical erosion) at the landscape surface. In contrast, mineral weathering can occur throughout the profile, implying that the other two (dominantly geochemical) frameworks share a broader range of locations within a profile, from the landscape surface down to the base of the deep CZ. Nevertheless, a considerable difference in scale separates the two geochemical frameworks. The mineral transformations that induce mass loss (i.e. chemical erosion) occur at the grain scale due to driving processes of advection and diffusion (encompassed by solute-transport and interface-limited mineral weathering). In contrast, measurements of chemical weathering fluxes out of pedons and catchments (encompassed by kinetic- and supply-limited chemical erosion) ultimately integrate both vertically and laterally over much larger spatial scales.

Despite the differences in scale and location of interest, the frameworks ultimately share the common goal of understanding rates of erosion and weathering in the CZ. Hence making connections between them is potentially powerful. For example, although the physical erosion framework was originally conceived by geomorphologists to interpret the relative importance of soil production and transport (Figure 3), it has also been used by geochemists to decipher contrasts in chemical erosion rates and geochemical properties of regolith (e.g. Stallard and Edmond, 1983). Under weathering-limited physical erosion, soils should be thin or absent, because the capacity for physical erosion is larger than the capacity for soil production (Figure 3); mobile soil vanishes before it has time to lose mass and thus exhibit extensive depletion (Figure 6), and effluxes of solutes are correspondingly devoid of all but the most soluble elements (Stallard and Edmond, 1983). Conversely, under transport-limited erosion, soil profiles should generally be thick, because soil production outpaces the capacity for removal, resulting in an increase in soil thickness (Figure 3). Thicker soils generally have longer residence times (Mudd and Yoo, 2010) and hence are relatively depleted in soluble elements (Figure 6), with effluxes of solutes that closely match molar ratios of elements in bedrock (Stallard and Edmond, 1983). In the Amazon, for example, solutes sourced from areas with the most intensely weathered regolith (in the transport-limited regime) have element ratios similar to parent bedrock, whereas solutes from areas with less intensively weathered regolith (in the weathering-limited regime) are enriched compared to parent bedrock both in sodium (Na) relative to potassium (K) and in calcium (Ca) relative to magnesium (Mg) (Stallard and Edmond, 1983).

Other useful connections can be made across disciplines. For example, on a transport-limited hillslope, where regolith profiles are thick and highly depleted, chemical erosion might be limited by the supply of weatherable minerals, consistent with the end-member regime of supply limitation in the chemical erosion framework (cf. Figures 6a and 6d). Meanwhile, on a weathering-limited hillslope, where regolith profiles are thin or absent, chemical erosion might be limited by the kinetics of weathering, consistent with the end-member regime of kinetic limitation in the chemical erosion framework (cf. Figures 6b and 6c). Thus the physical erosion framework (*sensu* Carson and Kirkby, 1972) can be useful in interpreting catchment-scale limitations on overall chemical erosion fluxes (West *et al.*, 2005) as well as differences in their elemental stoichiometry (Stallard and Edmond, 1983; West *et al.*, 2005).

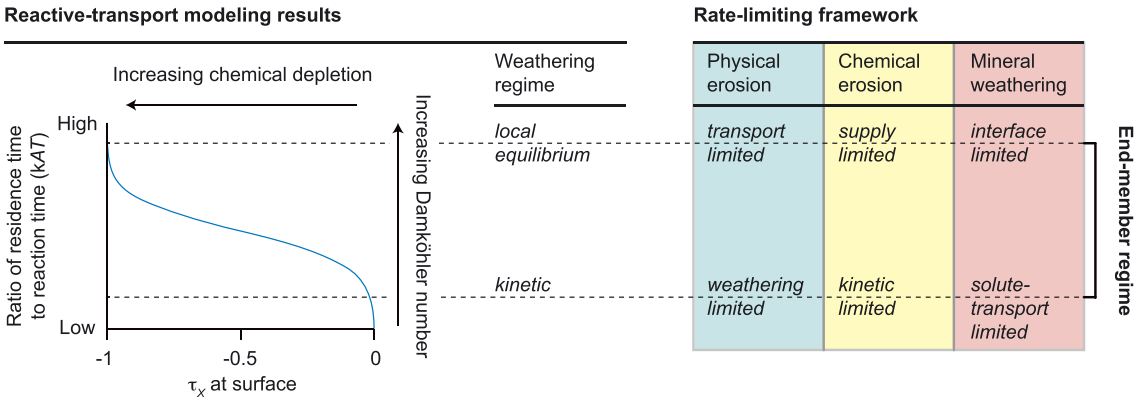

Figure 7. Connections between rate-limiting frameworks (right), illustrated with reactive-transport modeling results (left) for a mineral that has been carried from depth through the weathering profile by erosion at the surface. When regolith residence times (T_{reg}) are short compared to the mineral's reaction timescale ($k^{-1} A^{-1}$), the mineral is not completely lost due to weathering and can be found at the soil surface (lower dashed horizontal line across figure). This is the 'kinetic' weathering regime; mineral weathering is solute-transport limited, chemical erosion is kinetic limited, and physical erosion may be weathering limited. Conversely, when T_{reg} is long compared to $k^{-1} A^{-1}$, the reactive mineral is completely gone by the time soil reaches the surface (upper dashed line). This is the 'local equilibrium' regime. Here, chemical erosion is supply limited, physical erosion is likely transport limited, and mineral weathering is likely interface limited. [Colour figure can be viewed at wileyonlinelibrary.com]

The physical and chemical erosion frameworks can also be linked at the scale of individual pedons (i.e. a representative regolith profile in a catchment), as illustrated in reactive transport modeling (Lebedeva *et al.*, 2007; Brantley and White, 2009; Lebedeva *et al.*, 2010; Lebedeva and Brantley, 2013). In weathering-limited physical erosion, soils are thin, residence times are short, and modeling predicts that only the most soluble elements will be completely depleted from the profile because of the short residence time of minerals in the weathering zone. Elements that do become completely depleted have 'completely developed' profiles, with CDF = 1 at the surface, in the 'local equilibrium regime' (Figure 7). Elements that are not completely removed before they reach the land surface are in the 'kinetic regime', analogous to kinetic-limited chemical erosion and solute transport-limited mineral weathering (Figure 7). Conversely, in transport-limited physical erosion, soils are thick, residence times are long, and more elements may have completely developed weathering profiles, with CDF = 1 at the surface. Thus more minerals are reacting in the local equilibrium regime. For these minerals, chemical erosion is supply limited; the only way to increase the overall chemical erosion flux of the element from a completely developed soil profile is to increase its rate of supply to the weathering engine (i.e. the rate of conversion of rock to regolith). An analogy can also be made in such cases to an interface limitation on mineral weathering (Figure 7). In the field, this local equilibrium condition would manifest itself as soil profile in which the reacting mineral in question is not present at the land surface. Meanwhile, the kinetic case would manifest as a soil that retains at least a portion of the original mass of mineral at the land surface.

The linkages discussed earlier are qualitative, but they can also be expressed semi-quantitatively, in terms of the equations presented earlier. For example, if the ratio between the reaction rate constant (k in Equation (4)) and physical erosion efficiency (K in Equation (13)) is low, mineral weathering is likely to be solute-transport limited and chemical erosion is likely to be kinetic limited (Figure 7). Conversely, if k/K is high, mineral weathering is likely to be in the local equilibrium regime and chemical erosion fluxes are likely to be supply limited.

Unlike the expression for physical erosion rate (Equation (13)), the empirical soil-production function (Equation (10)) does not have a single coefficient for efficiency, complicating simple comparisons between these two rate-law formulations. However, it seems reasonable to suggest that when the maximum soil production rate (P_{max} in Equation (12)) is high relative to the erosional efficiency (K in Equation (10)), soils should generally be thick, with long residence times. These are hallmarks of soils undergoing transport-limited physical erosion (Figure 3). They may also be dominated by supply-limited chemical erosion, to the extent that thick soils with long residence times have mineral concentrations at the surface that show marked depletion relative to protolith (approaching the local equilibrium regime).

Insightful links can also be made between the mineral weathering and soil production rate equations. Mineral dissolution likely promotes and may also depend on soil production, such that the reaction rate constant (k in Equation (4)) and soil production rate (P in Equation (10)) are tightly coupled (e.g. Lebedeva and Brantley, 2013). For example, weathering in the local equilibrium regime due to high values of k might be expected to promote transport-limited physical erosion, wherein P is fast because dissolution and thus weakening of the bedrock or saprolite is also fast. Meanwhile kinetic-limited chemical erosion due to low values of k might be expected to induce weathering-limited physical erosion, wherein P_{max} is lower than the potential physical erosion rate (Figure 3) and soils are stripped to bare rock due to slow dissolution and weakening of bedrock. This provides a plausible mechanistic connection between the physical-erosion and mineral-weathering frameworks. These ideas are at the core of the modeling exercises described by Lebedeva and Brantley (2013) in this special issue.

Finally, we can arrive at additional quantitative connections between the mineral-weathering and chemical-erosion frameworks by comparing the characteristic reaction timescales of minerals $k^{-1}A^{-1}$ with the residence times of soil in the critical zone T_{reg}. The ratio of the latter to the former is kAT_{reg} which is analogous to the Damköhler number in Equation (16) (after Ferrier and Kirchner, 2008; Hilley *et al.*, 2010). When regolith residence times are short relative to the reaction timescale, kAT_{reg} is small, and chemical erosion is likely to be kinetic limited. When this is the case, the pedon will be in the kinetic regime and mineral weathering will be solute-transport limited (Figure 7). Physical erosion may be either weathering limited or transport limited under these conditions, because the connections between the mineral-weathering and chemical-erosion framework do not lead to an unequivocal determination of physical erosion regime.

One caveat to our semi-quantitative attempts at linking the frameworks is that the equations presented here for mineral weathering, sediment transport, and soil production are an illustrative but incomplete sampling of the many formulations that have been proposed in the literature over the years. It is therefore likely that other, even more insightful combinations of parameters can be posited for linking the frameworks across disciplines in different settings. In any case, more work is needed to explore the potential of linking the three rate-limiting frameworks discussed here. The connections that Stallard and Edmond (1983) and others (e.g. West *et al.*, 2005; Lebedeva *et al.*, 2010; Lebedeva and Brantley, 2013) have documented demonstrate that combinations of the conceptual frameworks can be useful and that more quantitative approaches are therefore worthy of future research.

Four Testable Hypotheses about Deep CZ Evolution

Our historical overview of CZ research highlights some of the many major advances that have been made over the last roughly five hundred years in understanding the coupled biogeochemical, hydrological and geomorphological processes that shape Earth's near-surface environment in mountain settings. It also calls attention to the relative lack of focus on the deep CZ in previous work, despite its clear importance in setting the template for more widely studied surface processes. Understanding of the processes that shape the deep CZ has remained largely out of reach until now due to the lack of a systematic effort to access the deep subsurface. However, recent developments – including several documented in this special issue – suggest that major advances are close at hand.

In this section, we highlight four testable hypotheses about the deep CZ that are emerging now from the USCZOs and other similar efforts around the world. Research on these hypotheses promises to improve understanding of controls on two of the most fundamental life-sustaining properties of the CZ: its overall thickness and the degree of weathering as a function of depth. We stress that this is not a comprehensive list of plausible hypotheses, but nonetheless hope that it may serve as a useful signpost for future process-based research on the deep CZ. A common theme across the hypotheses in our list is the importance of high-conductivity flowpaths and the introduction of reactive

meteoric fluids from the surface. The ease of access by surface waters, gases, and biota is undoubtedly related to the production and opening of fractures and pores and the dissolution of primary minerals in the deep CZ. Below we review the four hypotheses and discuss how they can be tested using observations from cores, boreholes and geophysical measurements.

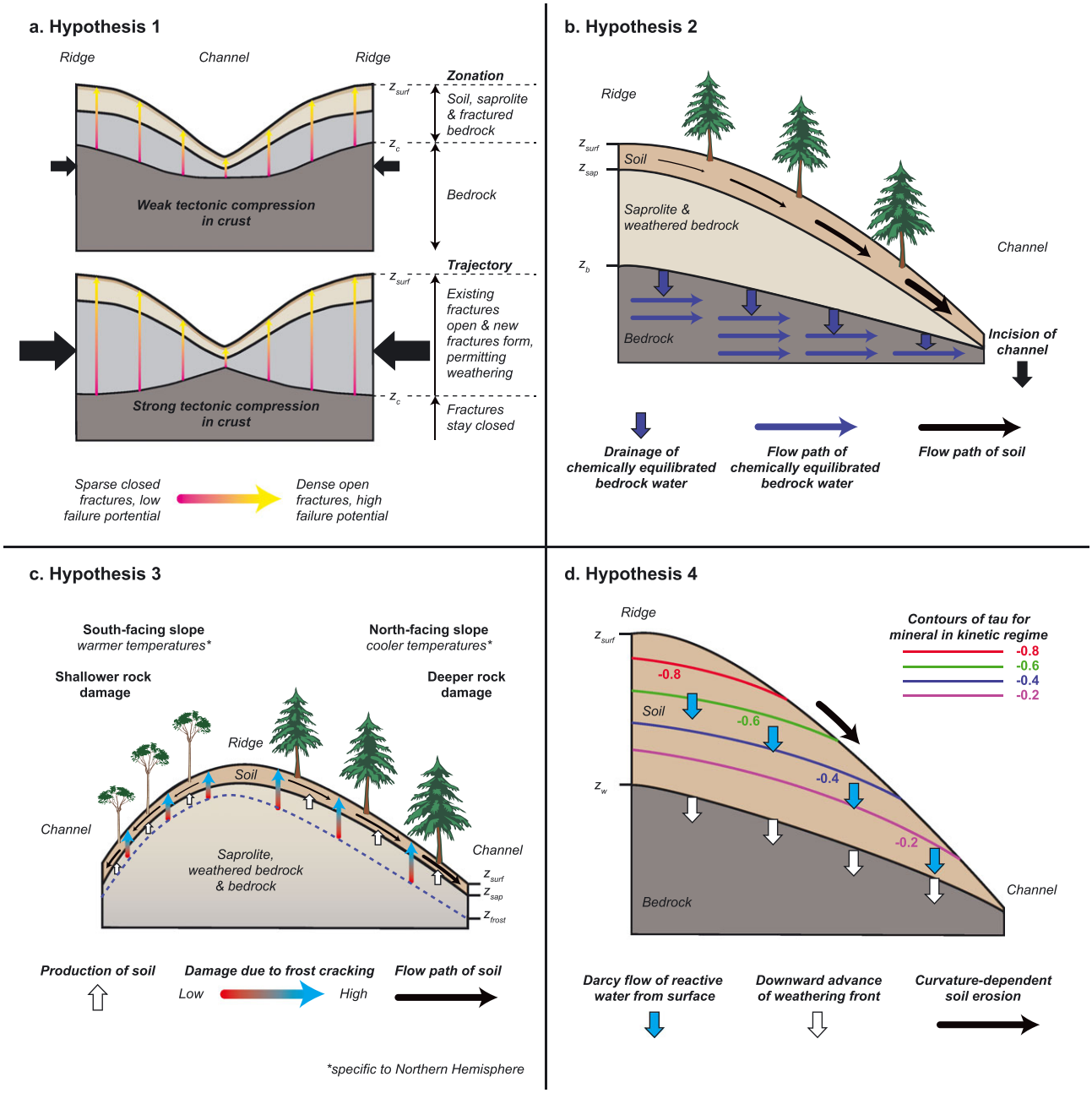

Figure 8. Four testable hypotheses about the evolution of the deep critical zone (CZ). Throughout this figure z_{surf} is the landscape surface; z_{sap} is the top of saprolite; z_{frost} is the base of rock damage due to frost cracking; z_b is the top of bedrock; z_w is the top of unweathered bedrock; and z_c is the base of the zone of open fractures in bedrock. (a) Hypothesis 1 is that topographic and tectonic stresses control the distribution of open fractures in the subsurface. Two endmember scenarios are illustrated (after Slim *et al.*, 2015; St Clair *et al.*, 2015): z_c should roughly parallel z_{surf} when compressive tectonic stresses in the crust are small relative to gravitational stresses caused by hilly topography (top image); meanwhile, z_c should mirror z_{surf} when compressive tectonic stresses are relatively large (bottom). Colored arrows in (a) show predicted gradients in failure potential and density of open fractures. Black arrows show relative strength of tectonic compression. (b) Hypothesis 2 is that drainage of chemically equilibrated pore fluids from bedrock initiates chemical weathering at the base of the CZ. Thick blue arrows denote bedrock drainage that exposes fresh bedrock to meteoric fluids at Z_b. Thin blue arrows show lateral flux of equilibrated waters in bedrock, consistent with the approximations used in the model for predicting z_b (Rempe and Dietrich, 2014). Black arrows show soil transport in mobile regolith which can be modeled using Equation (15) or a non-linear slope-dependent rate law (Rempe and Dietrich, 2014). (c) Hypothesis 3 is that climate and aspect-driven differences in frost cracking control variations in subsurface rock damage in the CZ. In the Northern Hemisphere, north-facing slopes experience colder temperatures, which lead to deeper rock damage due to frost cracking (Anderson *et al.*, 2013). This leads to a higher efficiency of both soil production (white arrows) and regolith flux (black arrows), which drives divide migration and a pronounced asymmetry of the ridge (Anderson *et al.*, 2013). (d) Hypothesis 4 is that erosion rates and fluid residence times control the thickness and degree of weathering of the CZ. Downward advection of reactive water from the surface drives mineral weathering via advection and diffusion, which in turn drive both vertical and lateral variations in element concentrations and thus tau, represented here with contour lines (after Lebedeva and Brantley, 2013). Steady-state soil thickness can be achieved by explicitly accounting for soil erosion (black arrow) as well as downward propagation of the weathering front via dissolution (white arrows). [Colour figure can be viewed at wileyonlinelibrary.com]

Hypothesis 1.

The distribution of subsurface weathering can be largely predicted from topographic and tectonic stresses and how they control the distribution of open fractures

Fractures are high-conductivity pathways that facilitate throughflow of reactive, non-equilibrated meteoric fluids and biota in the CZ. Thus they form a vital link between the surface and weathering at depth. The mechanical generation and opening of fractures is highly dependent on the subsurface stress field (Molnar *et al.*, 2007; Martel, 2011; Slim *et al.*, 2015), which varies across landscapes due to interactions between regional stresses that arise from plate tectonic forces and local gravitational stresses that arise from hilly topography (Slim *et al.*, 2015). Building on previous work, including the Slim *et al.* (2015) study published in this special issue, St Clair *et al.* (2015) showed how a simple metric of most- and least-compressive stresses can predict zones of high failure potential beneath landscapes, and thus zones of dense subsurface fracturing. We use z_c to refer to the elevation of the base of this predicted zone of high-density open fractures. Here, the subscript *c* denotes closure to significant infiltration of meteoric fluids and biota.

In landscapes where tectonic stresses are small relative to gravitational stresses from topography, subsurface stress calculations predict that z_c should be subparallel to the ground surface, rising in sync with it away from the channel (Figure 8a). Conversely, in landscapes where tectonic stresses are relatively large and compressive, the base of the densely fractured zone should mirror the surface topography, diving deeper into the subsurface away from the channel and creating a characteristic 'bowtie' shape (Figure 8a). Seismic refraction and resistivity surveys across sites with differing tectonic stress regimes have now documented a bowtie geometry of properties where tectonic compression is high and a subparallel geometry where tectonic compression is low (St Clair *et al.*, 2015). These observations, though limited to just three sites, are consistent with the hypothesis that topographic and tectonic stresses are a first order control on the lateral and vertical distribution of open fractures in the subsurface (St Clair *et al.*, 2015). More work is needed to test this hypothesis in other landscapes and to understand how subsurface fracture patterns contribute to weathering via the introduction of reactive meteoric fluids and biota. Key measurements should include: estimates of the integrated stress field (inferred from a combination of borehole breakout data and high-resolution surface topography); and both geophysical (i.e. indirect) and borehole (i.e. direct) measurements of near-surface fracturing and weathering.

Hypothesis 2.

Drainage of chemically equilibrated pore fluids initiates chemical weathering within bedrock

River incision dissects landscapes, driving hillslope erosion that exhumes unweathered bedrock along the CZ conveyor (Figure 2). Bedrock under a hillslope that is higher in elevation than its adjacent channel (Figure 8) experiences pressure head gradients that drive chemically equilibrated fluids out of the bedrock and towards the channel (Rempe and Dietrich, 2014). If this drainage of pore fluids is vital to exposing unweathered mineral surfaces to reactive meteoric waters from the surface, as proposed by Rempe and Dietrich (2014), it could be crucial to initiating bedrock weathering.

To model the drainage of bedrock pore water and ultimately predict z_b, the uppermost elevation of undrained bedrock, Rempe and Dietrich (2014) combined the regolith flux formula of Equation (15) with a lateral flow approximation of subsurface water. The predicted variations in the depth to undrained bedrock surface across a slope depend on several parameters, some of which, such as bedrock porosity and channel incision rate, can be measured or inferred fairly readily (e.g. Navarre-Sitchler *et al.*, 2015; Granger *et al.*, 1996), while others, such as hydraulic conductivity and soil diffusivity, are notoriously difficult to quantify. However, in landscapes where all of the parameters can be constrained, Rempe and Dietrich (2014) argue that the spatial distribution of z_b can be predicted and compared with geophysical and borehole-based measurements of deep CZ architecture. The agreement (or lack thereof) between predicted and observed z_b across the landscape represents one test of the hypothesis that the drainage of chemically equilibrated pore fluids initiates weathering in fresh bedrock.

Hypothesis 3.

Climate and aspect-driven differences in frost cracking control variations in subsurface rock damage in the CZ

Rock damage, which is defined as the weakening and eventual physical disaggregation (i.e. fracturing) of rock (Anderson *et al.*, 2013), promotes entrainment of material into the mobile soil, eases downslope transport of soil by reducing particle size, and also creates fluid flow paths that promote chemical weathering in soils and underlying rock. Rock can be damaged by many chemical and physical mechanisms as it approaches the surface, including fracturing due to stresses induced by oxidation reactions (Navarre-Sitchler *et al.*, 2015), tree roots (Roering *et al.*, 2010), and segregation ice growth, which can lead to frost cracking (Walder and Hallet, 1985; Hales and Roering, 2007).

In this special issue, Anderson *et al.* (2013) modeled rock damage due to frost cracking by integrating it over the time rock spends in the frost cracking window (−3 to −8 °C) during upward transport through the CZ, while also factoring in the distance liquid water must travel to the freezing front. As one outcome of their model, they proposed the hypothesis that climate and aspect-driven differences in frost cracking are strong predictors of the distribution of rock damage in the CZ and thus the rate of downslope soil transport (Figure 8c). Anderson *et al.* (2013) applied their model to the Boulder Creek CZO using depth profiles of temperature and aspect-driven variations in insolation to predict north–south asymmetries in rock damage that are broadly consistent with previous geophysical observations obtained by Befus *et al.* (2011). In general, the model predicts that z_{frost}, the depth of deepest rock damage due to frost cracking, should vary with hillslope aspect (Figure 8c), a prediction that can be tested in other landscapes with empirical or modeled temperature profiles and geophysical observations.

Hypothesis 4.

Erosion rates, fluid residence times, and mineral reactivities control the thickness and degree of weathering of the CZ

A fourth hypothesis emerges from considering the response of Earth materials to changing chemical conditions as they are exhumed to the surface. Meteoric fluids begin to react with primary rock minerals at some depth defined by z_w, the elevation of the inception of subsurface weathering. Above z_w, solute concentrations in fluids change until an equilibrium with surrounding minerals is approached. This process can be modeled using reactive-transport equations that simulate both advection and diffusion of solutes in a framework that accounts for variations in steady-state surface erosion rates and subsurface fluid residence times (e.g. Lichtner, 1988; Steefel *et al.*, 2005; Goddéris *et al.*, 2006; Lebedeva *et al.*, 2007, 2010; Maher, 2010).

Lebedeva and Brantley (2013) expanded on the one-dimensional (1D) (vertical) model of previous work by tracking the evolution of meteoric fluids towards equilibrium as they pass vertically through the CZ in a 2D slice through a hillslope (Figure 8d), parameterizing erosion rates as a function of surface curvature (cf. Equation (15)). Like the 1D model, the 2D model predicts that high chemical reaction rates or low physical erosion rates result in a local equilibrium condition (Figure 7) in which some mineral phases are completely dissolved away (tau = −1) during their time in the weathering zone. Meanwhile, when erosion rates are relatively high or when mineral-fluid reaction rates are relatively slow, many relatively reactive minerals can survive through the entire residence time of material in the subsurface CZ profile. This leads to the hypothesis that erosion rates, fluid residence times, and chemical reactivity (i.e. kinetics and solubility) control downward propagating chemical weathering fronts and thus regulate spatial variations in the thickness and degree of weathering of the CZ.

Predictions of the 2D model include increasing soil (i.e. mobile regolith) thickness with distance from the channel and variations in the concentration of different mineral phases as a function of depth for a physically unmixed soil (Figure 8d). In addition, the model emphasizes the importance of different mechanisms of solute transport, with distinct predictions for reaction fronts depending on whether reactions are dominated by diffusion or advection (Navarre-Sitchler *et al.*, 2015): in fast-dissolving rocks where solutes move via diffusion, reaction fronts are narrow and multiple minerals react together; meanwhile, in slow-dissolving rocks where solutes move via advection, reaction fronts are wider and differ in position within the rock for different minerals. These predictions can be tested with measurements of solid mineral phases across depth in cores and cuttings extracted from boreholes.

A synthesis of the four hypotheses

The geophysical, hydrologic, thermal, and geochemical phenomena that the four hypotheses emphasize as first-order controls on weathering can overlap considerably, because they are driven by overlapping gradients in stress, hydrostatic head, temperature, and chemical potential in the CZ. Interpretations of field observations and comparisons with model predictions can therefore be complicated by overprinted patterns of fracturing, bedrock drainage, rock damage, and weathering. Additional complications may arise from overprinting of biological processes, which are not explicitly emphasized in any of the hypotheses highlighted here, but are nonetheless undoubtedly important regulators of the extent of weathering in the deep CZ (e.g. Roering *et al.*, 2010), and could therefore be part of an additional hypothesis.

To appreciate the challenge of unravelling the relative importance of coupled controls on deep CZ architecture, consider for example the process of fracturing, which might be governed by both geophysical and geochemical factors. All landscapes experience the geophysical interactions between ambient tectonic and topographic stresses that produce variations in potential for subsurface fracturing. Thus the patterns predicted in Hypothesis 1 should be imprinted to a certain degree on deep CZ architecture everywhere. However, if bedrock has few pre-existing fractures (inherited from deeper in the crust), and if the subsurface stress field nowhere exceeds the critical value for shear failure, bedrock may remain largely free of fractures throughout its journey through the CZ, despite reduced overburden pressures during exhumation. This suggests that the mere absence of fractures in any one landscape is not a definitive general test of Hypothesis 1. Nor would the presence of fractures rule out the potentially strong influence of reactive transport induced weathering (Hypothesis 4), even when observed fractures follow patterns predicted by the topographic and tectonic stress regime. An alternate explanation that would need to be explored is that the fractures have developed in response to stress-corrosion cracking, which is generally referred to in the weathering literature as weathering-induced fracturing (Navarre-Sitchler *et al.*, 2015). Such fractures might develop, for example, due to the oxidation of biotite in the presence of carbon dioxide, oxygen and water from the surface (e.g. Bazilevskaya *et al.*, 2013) and might tend to be oriented in a pattern dictated by the subsurface stress field.

Additional complications arise when considering Hypothesis 3. Not all landscapes have climatic conditions favorable for frost cracking. In settings where frost cracking does occur, rock damage from this process may be limited to just the top few meters beneath the surface, where temperatures in the −3 to −8 °C window of segregation ice growth are possible (Anderson *et al.*, 2013). Thus frost cracking may often overprint upon other factors that affect the weathering profile, including chemical weathering, root wedging, and bioturbation (e.g. Gabet et al., 2003). One strength of frost-cracking models like the one proposed by Anderson *et al.* (2013) is that they can integrate the effects of rock damage over geologic time as subsurface temperature profiles change in response to changing climate (Anderson *et al.*, 2013; Rempel *et al.*, 2016). Thus it should be possible to directly account for paleoclimatic effects on rock damage due to frost cracking (Marshall *et al.*, 2015) when paleotemperatures in the subsurface can be reliably parameterized.

It is vital to recognize that the models at the core of the four hypotheses emphasize different processes and thus predict patterns in fundamentally different surfaces that may be related but need not (and may not often) match. For example, one might expect z_c, the elevation of fracturing from Hypothesis 1, to define the deepest surface given that the movement of meteoric fluids through open fractures is tantamount to moving the rock-fluid system away from equilibrium (Hypothesis 4). Because of this connection, however, z_c may often coincide closely with the deepest subsurface elevation of observable weathering, z_w. In general, we expect both z_c and z_w to be significantly deeper than z_{frost} (Hypothesis 3), which, when present, is closely coupled to temperatures at the land surface, and thus may be uppermost surface in the profile after z_{sap}, the elevation of the top of saprolite, which often occurs within a meter of the landscape surface (see Wald *et al.*, 2013). Meanwhile, the elevation of the undrained bedrock surface, z_b, likely lies somewhere between z_{sap} and z_c in many landscapes. This would be consistent with the rock drainage model of Rempe and Dietrich (2014), in which z_b under a hillslope can never be lower than it is under the channel due to the lateral flow approximation for chemically equilibrated water beneath z_b (Hypothesis 2). Thus the model of z_b (Figure 8b) predicts wedge-shaped zones of increasing overburden thickness towards the hillslope divide that do not reach below the elevation of the channel under any conditions, regardless of incision rate or tectonics. There are no such restrictions on the predicted depth to z_c or z_w. In fact, one of the hallmarks of Hypothesis 1 is that z_c should lie at the base of a bowtie-shaped zone of open fractures that reaches well below the elevation of the channel under ridges in regions of high tectonic compression (Figure 8a). A similar bow-tie pattern in the depth to z_w might arise due reactive transport along vertical and lateral flowpaths predicted by groundwater modeling in small catchments (e.g. Tóth, 1963); while such flowpaths have not yet been simulated in reactive transport modeling, they might generally lead to dissolution

under ridges and precipitation under channels, a pattern that might be consistent with bow-tie patterns of seismic velocities observed in some landscapes (St Clair *et al.*, 2015). More work is needed to explore this idea.

A conceptual model of fracturing and weathering in the deep CZ

The potential for overprinting of the geochemical and geophysical signatures of deep CZ processes highlights the importance of considering a combination of hypotheses when evaluating observations from cores, boreholes and geophysical surveys. Individually, the hypotheses highlighted here emphasize the effect of Earth materials moving upward through gradients in stress, temperature, hydrostatic head and chemical potential, which together define the CZ. This crossing of gradients provides a unifying theme that we use as the basis of the following integrative conceptual model of expected changes in fracturing, weathering, and fluid flow as bedrock is exhumed from depth by erosion at the surface:

Step 1 At some depth greater than z_c, fractures inherited by bedrock when it was deep in the crust – i.e. as it passed through the tectonic rock crusher of Molnar *et al.* (2007) – remain mostly closed to throughflowing meteoric water. However, beginning at z_c bedrock in the upward CZ conveyor experiences an ambient stress field that increasingly promotes both shear- and opening-mode failure within the rock (Figure 9). Across three crystalline bedrock sites where this depth has been inferred from subsurface stress modeling and seismic refraction surveys (St Clair *et al.*, 2015), it corresponds to P-wave velocities of ~4 km s^{-1}. Above this depth, existing fractures open, new fractures form, and the resulting increase in fracture porosity allows for entry of reactive fluids. In addition, the presence of reactive fluids may promote fracture development via stress-corrosion cracking. It is possible that z_c is generally deeper than z_w, or that z_w is generally co-located with z_c, or even, perhaps, that z_w is deeper than z_c – for example if unloading causes dilation of pores without fracturing and thus permits enough drainage for weathering to commence, despite the absence of fractures.

Step 2 As erosion at z_{surf} causes material to effectively rise through the zone above z_c and z_w, observed P-wave velocities decrease (St Clair *et al.*, 2015) as new fractures form via shear failure, as existing fractures begin to open up (Slim *et al.*, 2015; St. Clair *et al.*, 2015; Figure 9), and as chemical weathering continues (Brantley *et al.*, 2013). This promotes increased flow of meteoric water through the fracture network and promotes chemical reactions as reaction products are flushed away (Berner, 1978). However, if water is not flushed through very rapidly, weathering reactions will tend to be slow, diffusion dominated (Brantley and Lebedeva, 2011), and focused on fracture surfaces. If present in this zone, the position of the water table may be important because infiltrating oxygen (which can be fast in the vadose zone) can accelerate oxidation-induced fracturing, which may in turn promote more infiltration (Bazilevskaya *et al.*, 2013). Without significant fracturing and fluid flow, however, most minerals will weather in the kinetic regime characteristic of interface-limited mineral weathering (Figure 7). Only the most soluble minerals present at low abundance in the bedrock – such as accessory calcite in granite (White *et al.*, 1999b) – will be completely depleted and thus indicative of the local equilibrium regime (Lebedeva *et al.*, 2010).

Step 3 As the material in the CZ conveyor continues to rise under the landscape towards z_{surf}, the growing pressure-head gradient between the material and the adjacent channel may be sufficient to drive remaining chemically equilibrated bedrock pore water away from pores and into the channel (Rempe and Dietrich, 2014). The

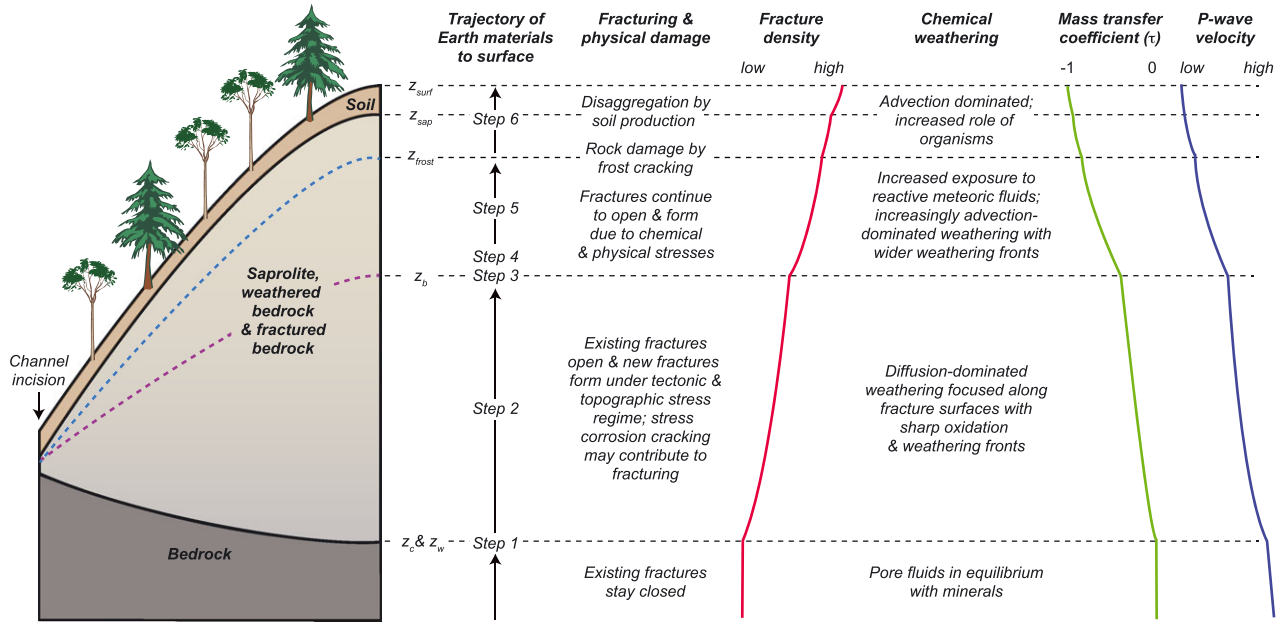

Figure 9. Conceptual model illustrating possible connections between the four hypotheses about the evolution of critical zone (CZ) architecture. Step numbers correspond to sequential changes in process and ambient conditions as Earth materials are exhumed from depth by erosion at the surface. Each of these steps are discussed in detail in the text. Hypothetical distributions of fracture density, mass transfer coefficient, and P-wave velocity as a function of depth show how variations in physical and chemical processes might be expressed in properties measured from boreholes, cores, drill cuttings and geophysical surveys of the deep CZ. [Colour figure can be viewed at wileyonlinelibrary.com]

elevation at this point in the material's upward trajectory is z_b (Figure 9).

Step 4 As the material traverses the zone immediately above z_b, pore surfaces exposed by drainage of bedrock pore fluids increasingly interact with meteoric fluids, including reactants such as oxygen and carbon dioxide from the surface (Rempe and Dietrich, 2014). This should promote an increase in weathering reactions, leading to steep gradients in both bulk geochemistry (e.g. tau) and geophysical characteristics such as the P-wave velocity (Figure 9). Weathering reactions are increasingly dominated by advection rather than diffusion here because the fraction of the material with low porosity and permeability becomes smaller as the density of fractures increases and as minerals begin to disaggregate from one another. Together, these changes reflect a transition from the solute-transport-limited to interface-limited mineral weathering.

Step 5 As the material rises still closer to the surface, the topographic and tectonic stress field continues to promote shear- and opening-mode failure in coherent blocks. Progressive mineral weathering due to reactive fluid transport is reflected in changes in tau as a function of depth for remaining minerals (Figure 9). Some minerals may be lost along the way, exhibiting completely developed profiles, with tau = −1 (Lebedeva *et al.*, 2010), indicative of supply-limited chemical erosion (Ferrier and Kirchner, 2008; Hilley *et al.*, 2010). Other minerals may remain and become exposed at the landscape surface, reflecting weathering in the kinetic regime (Lebedeva *et al.*, 2010). In some cases, material in the zone above z_b will experience fluctuating water table levels, which may promote oxidation and thus drive stress-corrosion fracturing that further increases the density of subsurface fractures. P-wave velocities of the subsurface should continue to decrease with increasing proximity to the surface (see for example Holbrook *et al.*, 2014).

Step 6 Near the top of the profile, in climates with sufficiently cold temperatures, frost cracking may impose an overprint of rock damage (Anderson *et al.*, 2013) on the fractures and weathering accrued via other processes at depth (Figure 9). Geophysical data may reflect this overprint (e.g. Befus *et al.*, 2011). However, interpretation may be complicated by the influence of biotic processes (Roering *et al.*, 2010; Anderson *et al.*, 2013) and the legacy of past climates (e.g. Anderson *et al.*, 2013; Marshall *et al.*, 2015). The highest surface in the profile is likely z_{sap}, the level at which saprolite is disaggregated by chemical, physical and biological processes into mobile soil particles.

A call to action

The conceptual model outlined above highlights four important surfaces within the deep and near-surface CZ: z_c, z_w, z_b, and z_{frost} (Figure 9). The proposed relationship among these surfaces is itself a testable hypothesis about how some of the processes discussed in this review link together to regulate subsurface architecture starting below the depth of closed fractures and following the trajectory of Earth materials all the way to the landscape surface. However, this model is by no means comprehensive. For example, it does not account for reactive transport along lateral subsurface flowpaths, which can be readily incorporated into numerical models of regolith production and hillslope evolution, as recent work has shown (Braun *et al.*, 2016). In addition, although our synthesis does quantitatively incorporates the influence of regional tectonics (Hypothesis 1), and different mineral reactivities (Hypothesis 4), there is no explicit treatment of lithologic effects on vegetation, erosion rates, and CZ thickness (e.g. Hahm *et al.*, 2014). Likewise, our synthesis does not include any bidirectional couplings between biota and CZ processes, which may often be profound (e.g. Hack and Goodlett, 1960; Brantley *et al.*, 2011). Future efforts could fill this conceptual gap by combining existing understanding of the effects of plant weathering (e.g. Kelly *et al.*, 1998; Moulton *et al.*, 2000), tree roots (e.g. Roering *et al.*, 2010; Gabet and Mudd, 2010; Pawlik, 2013), microbial communities (e.g. Balogh-Brunstad *et al.*, 2008) and ectomycorrhizal fungal networks (e.g. Bonneville et al., 2009) into an integrated hypothesis about feedbacks between biota and deep CZ architecture. Some progress on this topic was made in a recent synthesis of 12 hypotheses about the geobiology of weathering (Brantley *et al.* 2011), but more work is needed. In addition, we suggest that more work is needed to explore how other promising conceptual frameworks might be incorporated into deep CZ research. For example, a framework for incorporating effects of reactive transport along both vertical (Hypothesis 4) and lateral (Braun *et al.*, 2016) flowpaths is needed. An additional limitation of our synthesis is that it does not incorporate the concept of environmental energy and mass transfer (EEMT), which has come into increasingly widespread use in studies of water, carbon and energy and how they influence CZ processes (Rasmussen *et al.*, 2005, 2011a, 2015; Rasmussen and Tabor, 2007; Chorover *et al.*, 2011; Pelletier *et al.*, 2013). We suggest that development and testing of hypotheses related specifically to EEMT may be a fruitful avenue of future deep CZ research.

Drilling, sampling and imaging the deep CZ

Systematic lateral variations in the depth and degree of subsurface fracturing and weathering are the major hallmarks of the four hypotheses presented here (Figures 8 and 9). Hence, a vital first step in testing them will be to greatly expand the range of sites where deep subsurface properties have been measured. In particular, a coordinated campaign of drilling across a range of conditions (e.g. different climates and lithologies) will be needed to provide the geochemical and geophysical parameters used in model predictions. The US CZO network provides a potentially excellent testbed for such a sampling campaign, offering valuable leveraging opportunities from the many different CZ measurements that have been collected at each of the network sites over the last decade (e.g. Anderson *et al.*, 2008; Bales *et al.*, 2011; Chorover *et al.*, 2011; Kuntz *et al.*, 2011; Guo and Lin, 2016). However, because the deep CZ is highly heterogeneous, point samples from borehole observations, cuttings and cores will probably not be sufficient for comprehensive tests of the hypotheses. Quantifying the rich complexity of the deep CZ will require integration of new and existing geophysical and hydrologic techniques that interpolate between and extrapolate beyond information from boreholes for broad measures of fracturing, weathering, porosity and fluid flow at hillslope to catchment scales (e.g. Riebe and Chorover, 2014; Parsekian et al., 2015). Moving forward, it will be important to hone drilling and imaging techniques and sampling campaigns so that they systematically provide quantities needed to test the hypotheses. A concerted, community-wide effort on drilling, sampling and imaging of the deep CZ would help address the four hypotheses comprehensively.

Conclusions

To motivate this special issue on the deep CZ, we reviewed some of the many advances made over the last ~500 years in cross-disciplinary studies of weathering, erosion, and soil development. We began the review by defining the base of the CZ as the uppermost level in the near-surface environment where pore fluids in rock remain in thermodynamic equilibrium with adjacent high-pressure and high-temperature assemblages of minerals. One cross-cutting theme in our review is the vital role that quantitative studies of regolith production, erosion and weathering have played in documenting and understanding the factors that influence deep CZ processes. We compared and clarified the use of three historical frameworks for understanding rate limitations on (i) mineral weathering at the scale of individual mineral grains, (ii) physical erosion from mobile regolith, and (iii) chemical erosion from pedons and catchments. Examples from the literature were provided to illustrate how these frameworks have been coupled together in cross-disciplinary studies that span a range of spatiotemporal scales, from minerals to catchments and from seconds to millennia.

Looking forward, we highlighted four exciting hypotheses about the deep CZ that have recently emerged from across the US CZO network: (i) topographic and tectonic stresses control the distribution of open fractures in the subsurface; (ii) drainage of chemically equilibrated bedrock pore fluids initiates chemical weathering; (iii) climate and aspect-driven differences in frost cracking contribute to variations in subsurface rock damage in the CZ; (iv) erosion rates, fluid residence times, and mineral reactivities control the thickness and degree of weathering of the CZ. These hypotheses were motivated by process-based models of phenomena that vary across gradients in stress, hydraulic head, temperature, and chemical potential. They share as a common theme the importance of high-conductivity flow pathways and the introduction of reactive, non-equilibrated waters from the surface in determining the architecture of the deep CZ. Each of the hypotheses can be tested using observations from drilling, sampling and imaging. However, important limitations may arise in interpreting results when processes implicit in the different hypotheses overlap in time and space across the deep CZ.

Acknowledgments—The authors thank the editors of ESPL for the opportunity to organize this special issue and contribute this peer-reviewed synthesis. The editorial assistance and superhuman patience of Stuart Lane and Fiona Kirkby were greatly appreciated. The authors thank Bob Anderson, Bill Dietrich, Ken Ferrier, Steve Holbrook, Neil Humphrey, Mike Kirkby, Marina Lebedeva, Kate Maher, and Daniella Rempe for insightful discussions. Anonymous reviewer comments helped the authors clarify and focus the discussion. CSR acknowledges support from the Southern Sierra CZO (NSF EAR 0725097, 1239521 and 1331939) and the Wyoming Center for Environmental Hydrology and Geophysics (NSF EPS 1208909). WJH acknowledges support from the Roy J. Shlemon Center for Quaternary Studies at the University of Wyoming, the University of California Natural Reserve System Mildred E. Mathias Graduate Student Research Grant, and the Eel River CZO (NSF EAR 1331940). SLB acknowledges funding from the Department of Energy Office of Basic Energy Sciences grant DE-FG02-05ER15675 and from the Susquehanna/Shale Hills and Luquillo CZOs (NSF EAR 1339285 and 1331726 to S.L.B. and NSF EAR 1331841 to W.H. McDowell at the University of New Hampshire).

References

Ahnert F. 1967. The role of the equilibrium concept in the interpretation of landforms of fluvial erosion and deposition. *Presented at the Symposium International de Geomorphologie*, Liège-Louvain, 8–16 June 1966; 23–41.

Amundson RC. 2014. Soil formation. In *Treatise on Geochemistry*, Drever JI (ed). Elsevier: Oxford; 1–26.

Anderson DH, Hawkes HE. 1958. Relative mobility of the common elements in weathering of some schist and granite areas. *Geochimica et Cosmochimica Acta* **14**: 204–210.

Anderson RS, Humphrey NF. 1989. Interaction of weathering and transport processes in the evolution of arid landscapes. In *Quantitative Dynamic Stratigraphy*, Cross TA (ed). Prentice Hall: Upper Saddle River, NJ; 349–361.

Anderson RS, Anderson SP, Tucker GE. 2013. Rock damage and regolith transport by frost: an example of climate modulation of the geomorphology of the critical zone. *Earth Surface Processes and Landforms* **38**: 299–316.

Anderson SP, Bales RC, Duffy CJ. 2008. Critical Zone Observatories: Building a network to advance interdisciplinary study of Earth surface processes. *Mineralogical Magazine* **72**: 7–10.

Anderson SP, Blum J, Brantley SL, Chadwick O, Chorover J, Derry LA, Drever JI, Hering JG, Kirchner JW, Kump LR. 2004. Proposed initiative would study Earth's weathering engine. *Eos, Transactions American Geophysical Union* **85**: 265–272.

Anderson SP, Dietrich WE, Brimhall GH, Jr. 2002. Weathering profiles, mass-balance analysis, and rates of solute loss: Linkages between weathering and erosion in a small, steep catchment. *Geological Society of America, Bulletin* **114**: 1143–1158.

Anderson SP, von Blanckenburg F, White AF. 2007. Physical and chemical controls on the Critical Zone. *Elements* **3**: 315–319.

April R, Newton R, Coles LT. 1986. Chemical weathering in two Adirondack watersheds: Past and present-day rates. *Geological Society of America, Bulletin* **97**: 1232–1238.

Arkley RJ. 1981. Soil moisture use by mixed conifer forest in a summer-dry climate. *Soil Science Society of America Journal* **45**: 423–427.

Bales RC, Hopmans JW, O'Geen AT, Meadows M, Hartsough PC, Kirchner P, Hunsaker CT, Beaudette D. 2011. Soil moisture response to snowmelt and rainfall in a Sierra Nevada mixed-conifer forest. *Vadose Zone Journal* **10**: 786–799.

Balogh-Brunstad Z, Keller CK, Gill RA, Bormann BT, Li CY. 2008. The effect of bacteria and fungi on chemical weathering and chemical denudation fluxes in pine growth experiments. *Biogeochemistry* **88**: 153–167.

Bandstra JZ, Brantley SL. 2008. Data fitting techniques with applications to mineral dissolution kinetics. In *Kinetics of Water–Rock Interaction*, Brantley SL, Kubicki JD, White AF (eds). Springer: New York; 211–257.

Bandstra JZ, Buss HL, Campen RK, Liermann LJ, Moore J, Hausrath EM, Navarre-Sitchler AK, Brantley SL. 2008. Appendix: compilation of mineral dissolution rates. In *Kinetics of Water–Rock Interaction*, Brantley SL, Kubicki JD, White AF (eds). Springer: New York; 737–823.

Banfield JF, Barker WW, Welch SA, Taunton AE. 1999. Biological impact on mineral dissolution: application of the lichen model to understanding mineral weathering in the rhizosphere. *Proceedings of the National Academy of Sciences* **96**: 3404–3411.

Banwart S, Bernasconi SM, Bloem J, Blum W, Brandao M, Brantley SL, Chabaux F, Duffy C, Kram P, Lair G, Lundin L, Nikolaidis N, Novak M, Panagos P, Ragnarsdottir KV, Reynolds BC, Rousseva S, de Ruiter P, van Gaans P, van Riemsdijk W, White T, Zhang B. 2011. Soil processes and functions in critical zone observatories: hypotheses and experimental design. *Vadose Zone Journal* **10**: 974–987.

Bazilevskaya E, Lebedeva MI, Pavich MJ, Rother G, Parkinson DY, Cole D, Brantley SL. 2013. Where fast weathering creates thin regolith and slow weathering creates thick regolith. *Earth Surface Processes and Landforms* **38**: 847–858.

Becker GF. 1895. Reconnaissance of the Gold Fields of the Southern Appalachians. In *Extract from the Sixteenth Annual Report of the Director, 1894–95. Part II – Mineral Resources of the United States Calendar Year 1894*. US Department of the Interior, Geological Survey: Washington, DC.

Befus KM, Sheehan AF, Leopold M, Anderson SP, Anderson RS. 2011. Seismic constraints on critical zone architecture, Boulder Creek Watershed, Front Range, Colorado. *Vadose Zone Journal* **10**: 915–927.

Belt T. 1874. *The Naturalist in Nicaragua*. University of Chicago Press: Chicago, IL.

Bern CR, Chadwick OA, Hartshorn AS, Khomo LM, Chorover J. 2011. A mass-balance model to separate and quantify colloidal and solute redistributions in soil. *Chemical Geology* **282**: 113–119.

Bern CR, Thompson A, Chadwick OA. 2015. Quantification of colloidal and aqueous element transfer in soils: the dual-phase mass balance model. *Geochimica et Cosmochimica Acta* **151**: 1–18.

Berner EK, Berner RA, Moulton K. 2003. Plants and mineral weathering: present and past. In *Treatise on Geochemistry*, Drever JI (ed). Elsevier: Oxford; 169–188.

Berner RA. 1978. Rate control of mineral dissolution under Earth surface conditions. *American Journal of Science* **278**: 1235–1252.

Berner RA. 2012. Jacques-Joseph Ebelmen, the founder of earth system science. *Comptes Rendus Geoscience* **344**: 544–548.

Berner RA, Lasaga AC, Garrels RM. 1983. The carbonate–silicate geochemical cycle and its effect on atmospheric carbon-dioxide over the past 100 million years. *American Journal of Science* **283**: 641–683.

Bierman PR, Steig EJ. 1996. Estimating rates of denudation using cosmogenic isotope abundances in sediment. *Earth Surface Processes and Landforms* **21**: 125–139.

Bischof G. 1863. *Lehrbuch der chemischen und physikalischen Geologie*. Adoph Marus: Bonn.

Bluth GJS, Kump LR. 1994. Lithologic and climatologic controls of river chemistry. *Geochimica et Cosmochimica Acta* **58**: 2341–2359.

Bonneville S, Smits MM, Brown A, Harrington J, Leake JR, Brydson R, Benning LG. 2009. Plant-driven fungal weathering: early stages of mineral alteration at the nanometer scale. *Geology* **37**: 615–618.

Brantley SL, Lebedeva MI. 2011. Learning to read the chemistry of regolith to understand the Critical Zone. *Annual Review of Earth and Planetary Sciences* **39**: 387–416.

Brantley SL, Olsen AA. 2014. Reaction kinetics of primary rock-forming minerals under ambient conditions. In *Treatise on Geochemistry*, Drever JI (ed). Elsevier: Oxford; 69–113.

Brantley SL, White AF. 2009. Approaches to modeling weathered regolith. *Reviews in Mineralogy and Geochemistry* **70**: 435–484.

Brantley SL, Crane SR, Crerar DA, Hellmann R, Stallard R. 1986. Dissolution at dislocation etch pits in quartz. *Geochimica et Cosmochimica Acta* **50**: 2349–2361.

Brantley SL, Goldhaber MB, Ragnarsdottir KV. 2007a. Crossing disciplines and scales to understand the Critical Zone. *Elements* **3**: 307–314.

Brantley SL, Holleran ME, Jin L, Bazilevskaya E. 2013. Probing deep weathering in the Shale Hills Critical Zone Observatory, Pennsylvania (USA): the hypothesis of nested chemical reaction fronts in the subsurface. *Earth Surface Processes and Landforms* **38**: 1280–1298.

Brantley SL, Lebedeva M, Bazilevskaya E. 2014. Relating weathering fronts for acid neutralization and oxidation to pCO2 and pO2. In *Treatise on Geochemistry*, Farquhar J, Kasting J, Canfield D (eds). Elsevier: Amsterdam; 327–352.

Brantley SL, Megonigal JP, Scatena FN, Balogh-Brunstad Z, Barnes RT, Bruns MA, Van Cappellen P, Dontsova K, Hartnett HE, Hartshorn AS, Heimsath AM, Herndon EM, Jin L, Keller CK, Leake JR, McDowell WH, Meinzer FC, Mozdzer TJ, Petsch S, Pett-Ridge J, Pregitzer KS, Raymond PA, Riebe CS, Shumaker K, Sutton-Grier A, Walter R, Yoo K. 2011. Twelve testable hypotheses on the geobiology of weathering. *Geobiology* **9**: 140–165.

Brantley SL, White TS, Ragnarsdottir KV. 2007b. The critical zone: where rock meets life. *Elements* **3**: 5.

Brantley SL, White TS, White AF, Sparks DL, deB Richter D, Pregitzer KS, Derry LA, Chorover J, Chadwick OA, April R, Anderson SP, Amundson RC. 2006. Frontiers in exploration of the critical zone. *Report of a Workshop Sponsored by the National Science Foundation (NSF)*, 24–26 October 2005, Newark, DE.

Braun J, Mercier J, Guillocheau F, Robin C. 2016. A simple model for regolith formation by chemical weathering. *Journal of Geophysical Research: Earth Surface*: 1–81. DOI:10.1002/2016JF003914.

Brewer R. 1964. *Fabric and Mineral Analysis of Soils*. John Wiley & Sons: New York.

Bricker OP, Godfrey AE, Cleaves ET. 1968. Mineral–water interaction during the chemical weathering of silicates. In *Trace Inorganics in Water*, Baker RA (ed). American Chemical Society: Washington, DC; 128–142.

Bricker OP, Jones BF, Browser CJ. 2003. Mass-balance approach to interpreting weathering reactions in watershed systems. In *Treatise on Geochemistry*, Drever JI (ed). Elsevier: Oxford; 119–132.

Brimhall GH, Jr, Dietrich WE. 1987. Constitutive mass balance relations between chemical composition, volume, density, porosity, and strain in metasomatic hydrochemical systems: results on weathering and pedogenesis. *Geochimica et Cosmochimica Acta* **51**: 567–587.

Brimhall GH, Jr, Chadwick OA, Lewis CJ, Compston W, Williams IS, Danti KJ, Dietrich WE, Power ME, Hendricks D, Bratt J. 1992. Deformational mass-transport and invasive processes in soil evolution. *Science* **255**: 695–702.

Brimhall GH, Jr, Lewis CJ, Ford C, Bratt J, Taylor G, Warin O. 1991. Quantitative geochemical approach to pedogenesis – importance of parent material reduction, volumetric expansion, and eolian influx in lateritization. *Geoderma* **51**: 51–91.

Brown ET, Stallard RF, Larsen MC, Raisbeck GM, Yiou F. 1995. Denudation rates determined from the accumulation of *in situ*-produced Be-10 in the Luquillo Experimental Forest, Puerto-Rico. *Earth and Planetary Science Letters* **129**: 193–202.

Burke BC, Heimsath AM, Dixon JL, Chappell J, Yoo K. 2009. Weathering the escarpment: chemical and physical rates and processes, south-eastern Australia. *Earth Surface Processes and Landforms* **34**: 768–785.

Burke BC, Heimsath AM, White AF. 2007. Coupling chemical weathering with soil production across soil-mantled landscapes. *Earth Surface Processes and Landforms* **32**: 853–873.

Buss HL, Brantley SL, Scatena FN, Bazilievskaya EA, Blum AE, Schulz M, Jiménez R, White AF, Rother G, Cole DR. 2013. Probing the deep critical zone beneath the Luquillo Experimental Forest, Puerto Rico. *Earth Surface Processes and Landforms* **38**: 1170–1186.

Buss HL, Mathur R, White AF, Brantley SL. 2010. Phosphorus and iron cycling in deep saprolite, Luquillo Mountains, Puerto Rico. *Chemical Geology* **269**: 52–61.

Buss HL, Sak P, Webb S, Brantley SL. 2008. Weathering of the Rio Blanco quartz diorite, Luquillo Mountains, Puerto Rico: coupling oxidation, dissolution, and fracturing. *Geochimica et Cosmochimica Acta* **72**: 4488–4507.

Calmels D, Galy A, Hovius N, Bickle MJ, West AJ, Chen M-C, Chapman HJ. 2011. Contribution of deep groundwater to the weathering budget in a rapidly eroding mountain belt, Taiwan. *Earth and Planetary Science Letters* **303**: 48–58.

Carson MA, Kirkby MJ. 1972. *Hillslope Form and Process*. Cambridge University Press: London.

Chabaux F, Blaes E, Stille P, di Chiara RR, Pelt E, Dosseto AJ, Ma L, Buss HL, Brantley SL. 2013. Regolith formation rate from U-series nuclides: implications from the study of a spheroidal weathering profile in the Rio Icacos watershed (Puerto Rico). *Geochimica et Cosmochimica Acta* **100**: 73–95.

Chabaux F, Bourdon B, Riotte J. 2008. U-series geochemistry in weathering profiles, river waters and lakes. *Radioactivity in the Environment* **13**: 49–101.

Chadwick OA, Brimhall GH, Jr, Hendricks DM. 1990. From a black to a gray box – a mass balance interpretation of pedogenesis. *Geomorphology* **3**: 369–390.

Chadwick OA, Roering JJ, Heimsath AM, Levick SR, Asner GP, Khomo L. 2013. Shaping post-orogenic landscapes by climate and chemical weathering. *Geology* **41**: 1171–1174.

Chorover J, Kretzschmar R, Garcia-Pichel F, Sparks DL. 2007. Soil biogeochemical processes within the Critical Zone. *Elements* **3**: 321–326.

Chorover J, Troch PA, Rasmussen C, Brooks PD, Pelletier JD, Breshars DD, Huxman TE, Kurc SA, Lohse KA, McIntosh JC, Meixner T, Schaap MG, Litvak ME, Perdrial J, Harpold A, Durcik M. 2011. How water, carbon, and energy drive critical zone evolution: the Jemez-Santa Catalina Critical Zone Observatory. *Vadose Zone Journal* **10**: 884–899.

Clayton JL, Arnold JF. 1972. Practical Grain Size, Fracturing Density, and Weathering Classification of Intrusive Rocks of the Idaho Batholith, USDA Forest Service General Technical Report INT-2. US Department of Agriculture: Washington, DC.

Cleaves ET, Godfrey AE, Bricker OP. 1970. Geochemical balance of a small watershed and its geomorphic implications. *Geological Society of America, Bulletin* **81**: 3015–3032.

Clow DW, Drever JI. 1996. Weathering rates as a function of flow through an alpine soil. *Chemical Geology* **132**: 131–141.

Cox NJ. 1980. On the relationship between bedrock lowering and regolith thickness. *Earth Surface Processes and Landforms* **5**: 271–274.

Cremeens DL, Brown RB, Huddleston JH. 1994. *Whole Regolith Pedology*, SSSA Special Publication 34. SSSA; Madison, WI.

Culling WEH. 1960. Analytical theory of erosion. *Journal of Geology* **68**: 336–344.

Culling WEH. 1963. Soil creep and the development of hillside slopes. *Journal of Geology* **71**: 127–161.

Darwin C. 1876. *Geological Observations on the Volcanic Islands and Parts of South America Visited during the Voyage of the HMS 'Beagle.'* Smith and Elders: London.

Davis WM. 1892. The convex profile of bad-land divides. *Science* **20**: 245–245.

Dethier DP. 1986. Weathering rates and the chemical flux from catchments in the Pacific Northwest, USA. In *Rates of Chemical Weathering of Rocks and Minerals*, Coleman SM, Dethier DP (eds). Academic Press: Orlando, FL; 503–530.

Dethier DP, Lazarus ED. 2006. Geomorphic inferences from regolith thickness, chemical denudation and CRN erosion rates near the glacial limit, Boulder Creek catchment and vicinity, Colorado. *Geomorphology* **75**: 384–399.

Dietrich WE, Perron JT. 2006. The search for a topographic signature of life. *Nature* **439**: 411–418.

Dietrich WE, Bellugi DG, Sklar LS, Stock JD, Heimsath AM, Roering JJ. 2003. Geomorphic Transport Laws for Predicting Landscape Form and Dynamics. In *Prediction in Geomorphology, Geophysical Monograph Series 135*, Wilcock PR, Iverson RM (eds). American Geophysical Union: Washington, DC; 103–132.

Dietrich WE, Reiss R, Hsu ML, Montgomery DR. 1995. A process-based model for colluvial soil depth and shallow landsliding using digital elevation data. *Hydrological Processes* **9**: 383–400.

Dixon JL, Riebe CS. 2014. Tracing and pacing soil across slopes. *Elements* **10**: 363–368.

Dixon JL, von Blanckenburg F. 2012. Soils as pacemakers and limiters of global silicate weathering. *Comptes Rendus Geoscience* **344**: 597–609.

Dixon JL, Hartshorn AS, Heimsath AM, DiBiase RA, Whipple KX. 2012. Chemical weathering response to tectonic forcing: A soils perspective from the San Gabriel Mountains, California. *Earth and Planetary Science Letters* **323**: 40–49.

Dixon JL, Heimsath AM, Amundson RC. 2009. The critical role of climate and saprolite weathering in landscape evolution. *Earth Surface Processes and Landforms* **34**: 1507–1521.

Dokuchaev VV. 1967. Russian Chernozem. In *Selected Works of V.V. Dokuchaev*. Israel Program for Scientific Translations: Jerusalem.

Dosseto A, Buss HL, Chabaux F. 2014. Age and weathering rate of sediments in small catchments: the role of hillslope erosion. *Geochimica et Cosmochimica Acta* **132**: 238–258.

Dosseto AJ, Bourdon B, Gaillardet J, Allègre CJ, Filizola N. 2006. Time scale and conditions of weathering under tropical climate: Study of the Amazon basin with U-series. *Geochimica et Cosmochimica Acta* **70**: 71–89.

Dosseto AJ, Buss HL, Suresh PO. 2012. Rapid regolith formation over volcanic bedrock and implications for landscape evolution. *Earth and Planetary Science Letters* **337–338**: 47–55.

Dosseto AJ, Turner SP, Chappell J. 2008. The evolution of weathering profiles through time: new insights from uranium-series isotopes. *Earth and Planetary Science Letters* **274**: 359–371.

Drever JI. 1994. The effect of land plants on weathering rates of silicate minerals. *Geochimica et Cosmochimica Acta* **58**: 2325–2332.

Drever JI, Zobrist J. 1992. Chemical weathering of silicate rocks as a function of elevation in the southern Swiss Alps. *Geochimica et Cosmochimica Acta* **56**: 3209–3216.

Dunne T. 1978. Rates of chemical denudation of silicate rocks in tropical catchments. *Nature* **274**: 244–246.

Ebelmen JJ. 1845. Sur les produits de la décomposition des espèces minérales de la famille des silicates. *Annales des Mines* **7**: 3–66.

Elmore D, Phillips FM. 1987. Accelerator mass spectrometry for measurement of long-lived radioisotopes. *Science* **236**: 543–550.

Feller C, Blanchart E, Yaalon DH. 2006. Some major scientists (Palissy, Buffon, Thaer, Darwin and Muller) have described soil profiles and developed soil survey techniques before 1883. In *Footprints in the Soil: People and Ideas in Soil History*, Warkentin BP (ed). Elsevier: Amsterdam; 85–105.

Ferrier KL, Kirchner JW. 2008. Effects of physical erosion on chemical denudation rates: a numerical modeling study of soil-mantled hillslopes. *Earth and Planetary Science Letters* **272**: 591–599.

Ferrier KL, Kirchner JW, Finkel RC. 2011. Estimating millennial-scale rates of dust incorporation into eroding hillslope regolith using cosmogenic nuclides and immobile weathering tracers. *Journal of Geophysical Research* **116**: 1–11.

Ferrier KL, Kirchner JW, Riebe CS, Finkel RC. 2010. Mineral-specific chemical weathering rates over millennial timescales: measurements at Rio Icacos, Puerto Rico. *Chemical Geology* **277**: 101–114.

Ferrier KL, Riebe CS, Hahm WJ. 2016. Testing for supply-limited and kinetic-limited chemical erosion in field measurements of regolith production and chemical depletion. *Geochemistry, Geophysics, Geosystems* **17**: 2270–2285.

Feth JH, Roberson CE, Polzer WL. 1964. *Sources of Mineral Constituents in Water from Granitic Rocks: Sierra Nevada, California and Nevada*. US Government Printing Office: Washington, DC.

Fletcher RC, Brantley SL. 2010. Reduction of bedrock blocks as corestones in the weathering profile: observations and model. *American Journal of Science* **310**: 131–164.

Fournet MJ. 1833. Memoire sur la decomposition des minerais d'origine ignee et leur conversion en kaolin. *Annales de Chimie et de Physique* **LV**: 240–256.

Furbish DJ, Haff PK, Dietrich WE, Heimsath AM. 2009. Statistical description of slope-dependent soil transport and the diffusion-like coefficient. *Journal of Geophysical Research* **114**: F00A05.

Gabet EJ. 2007. A theoretical model coupling chemical weathering and physical erosion in landslide-dominated landscapes. *Earth and Planetary Science Letters* **264**: 259–265.

Gabet EJ, Mudd SM. 2009. A theoretical model coupling chemical weathering rates with denudation rates. *Geology* **37**: 151–154.

Gabet EJ, Mudd SM. 2010. Bedrock erosion by root fracture and tree throw: a coupled biogeomorphic model to explore the humped soil production function and the persistence of hillslope soils. *Journal of Geophysical Research* **115**: 1–14. DOI:10.1029/2009JF001526.

Gabet EJ, Reichman OJ, Seabloom E. 2003. The effects of bioturbation on soil processes and sediment transport. *Annual Review of Earth and Planetary Sciences* **31**: 249–273.

Gaillardet J, Dupre B, Louvat P, Allègre CJ. 1999. Global silicate weathering and CO2 consumption rates deduced from the chemistry of large rivers. *Chemical Geology* **159**: 3–30.

Galvez ME, Gaillardet J. 2012. Historical constraints on the origins of the carbon cycle concept. *Comptes Rendus Geoscience* **344**: 549–567.

Garrels RM, Mackenzie FT. 1967. Origin of the chemical compositions of some springs and lakes. In *Equilibrium Concepts in Natural Water Systems*, Stumm W (ed). American Chemical Society: Washington, DC; 222–242.

Gilbert GK. 1877. *Report on the Geology of the Henry Mountains*. Department of the Interior: Washington, DC.

Gilbert GK. 1909. The convexity of hilltops. *Journal of Geology* **17**: 344–350.

Gíslason SR, Eugster HP. 1987. Meteoric water-basalt interactions. II: A field study in N.E. Iceland. *Geochimica et Cosmochimica Acta* **51**: 2841–2855.

Goddéris Y, Brantley SL. 2014. Earthcasting the future Critical Zone. *Elementa* **1**: 000019. DOI:10.12952/journal.elementa.000019.

Goddéris Y, François LM, Probst A, Schott J, Moncoulon D, Labat D, Viville D. 2006. Modelling weathering processes at the catchment scale: The WITCH numerical model. *Geochimica et Cosmochimica Acta* **70**: 1128–1147.

Goldich SS. 1938. A study in rock-weathering. *Journal of Geology* **46**: 17–58.

Goodfellow B, Chadwick OA, Hilley G. 2014. Depth and character of rock weathering across a basaltic-hosted climosequence on Hawai'i. *Earth Surface Processes and Landforms* **39**: 381–398.

Goulden ML, Anderson RG, Bales RC, Kelly AE, Meadows M, Winston GC. 2012. Evapotranspiration along an elevation gradient in California's Sierra Nevada. *Journal of Geophysical Research* **117**: G03028–G03709. DOI:10.1029/2012JG002027.

Graham RC, Rossi A, Hubbert KR. 2010. Rock to regolith conversion: producing hospitable substrates for terrestrial ecosystems. *GSA Today* **20**: 4–9.

Graham RC, Tice KR, Guertal WR. 1994. The pedologic nature of weathered rock. In *Whole Regolith Pedology*, Cremeens DL, Brown RB, Huddleston, JH (eds), SSSA Special Publication 34. SSSA; Madison, WI; 21–40.

Graly JA, Bierman PR, Reusser LJ, Pavich MJ. 2010. Meteoric ^{10}Be in soil profiles – a global meta-analysis. *Geochimica et Cosmochimica Acta* **74**: 6814–6829.

Granger DE, Riebe CS. 2014. Cosmogenic nuclides in erosion and weathering. In *Treatise on Geochemistry*, Drever JI (ed). Elsevier: Oxford; 401–436.

Granger DE, Kirchner JW, Finkel RC. 1996. Spatially averaged long-term erosion rates measured from *in situ*-produced cosmogenic nuclides in alluvial sediment. *Journal of Geology* **104**: 249–257.

Green EG, Dietrich WE, Banfield JF. 2006. Quantification of chemical weathering rates across an actively eroding hillslope. *Earth and Planetary Science Letters* **242**: 155–169.

Guo L, Lin H. 2016. Critical zone research and observatories: Current status and future perspectives. *Vadose Zone Journal* **15**: 1–14. DOI:10.2136/vzj2016.06.0050.

Hack JT. 1960. Interpretation of erosional topography in humid temperate regions. *American Journal of Science* **258**: 80–97.

Hack JT, Goodlett JC. 1960. Geomorphology and Forest Ecology of a Mountain Region in the Central Appalachians, US Geological Survey Professional Paper 347. US Department of the Interior: Washington, DC; 1–66.

Hahm WJ, Riebe CS, Lukens CE, Araki S. 2014. Bedrock composition regulates mountain ecosystems and landscape evolution. *Proceedings of the National Academy of Sciences* **111**: 3338–3343.

Hales TC, Roering JJ. 2005. Climate-controlled variations in scree production, Southern Alps, New Zealand. *Geology* **33**: 701–704.

Hales TC, Roering JJ. 2007. Climatic controls on frost cracking and implications for the evolution of bedrock landscapes. *Journal of Geophysical Research* **112**: 1–14.

Hartt CF. 1853. *Geologia e geografia fisica do Brasil*. Companhia Editoria Nacional: Sao Paola.

Heimsath AM, Chappell J, Dietrich WE, Nishiizumi K, Finkel RC. 2000. Soil production on a retreating escarpment in southeastern Australia. *Geology* **28**: 787–790.

Heimsath AM, DiBiase RA, Whipple KX. 2012. Soil production limits and the transition to bedrock-dominated landscapes. *Nature Geoscience* **5**: 210–214.

Heimsath AM, Dietrich WE, Nishiizumi K, Finkel RC. 1997. The soil production function and landscape equilibrium. *Nature* **388**: 358–361.

Heimsath AM, Dietrich WE, Nishiizumi K, Finkel RC. 1999. Cosmogenic nuclides, topography, and the spatial variation of soil depth. *Geomorphology* **27**: 151–172.

Heimsath AM, Furbish DJ, Dietrich WE. 2005. The illusion of diffusion: field evidence for depth-dependent sediment transport. *Geology* **33**: 949–952.

Hilley GE, Porder S. 2008. A framework for predicting global silicate weathering and CO_2 drawdown rates over geologic time-scales. *Proceedings of the National Academy of Sciences* **105**: 16855–16859.

Hilley GE, Chamberlain CP, Moon S, Porder S, Willett SD. 2010. Competition between erosion and reaction kinetics in controlling silicate-weathering rates. *Earth and Planetary Science Letters* **293**: 191–199.

Holbrook WS, Riebe CS, Elwaseif M, Hayes JL, Reeder K, Harry DL, Malazian A, Dosseto AJ, Hartsough PC, Hopmans JW. 2014. Geophysical constraints on deep weathering and water storage potential in the Southern Sierra Critical Zone Observatory. *Earth Surface Processes and Landforms* **39**: 366–380.

Howard AD. 1994. A detachment-limited model of drainage-basin evolution. *Water Resources Research* **30**: 2261–2285.

Hren MT, Hilley GE, Chamberlain CP. 2007. The relationship between tectonic uplift and chemical weathering rates in the Washington Cascades: field measurements and model predictions. *American Journal of Science* **307**: 1041–1063.

Hubbert KR, Graham RC, Anderson MA. 2001. Soil and weathered bedrock: components of a Jeffrey pine plantation substrate. *Soil Science Society of America Journal* **65**: 1255–1262.

Hug LA, Baker BJ, Anantharaman K, Brown CT, Probst AJ, Castelle CJ, Butterfield CN, Hernsdorf AW, Amano Y, Ise K, Suzuki Y, Dudek N, Relman DA, Finstad KM, Amundson R, Thomas BC, Banfield JF. 2016. A new view of the tree of life. *Nature Microbiology* **1**: 16048. DOI:10.1038/nmicrobiol.2016.48.

Humphreys GS, Wilkinson MT. 2007. The soil production function: a brief history and its rediscovery. *Geoderma* **139**: 73–78.

Hunt TS. 1874. On the crystalline rocks of the Blue Ridge. *Proceedings of the Boston Society of Natural History*. AA Kingman: Boston, MA; 115–117.

Hurst MD, Mudd SM, Walcott R, Attal M, Yoo K. 2012. Using hilltop curvature to derive the spatial distribution of erosion rates. *Journal of Geophysical Research* **117**: 1–19, F02017.

Hurst MD, Mudd SM, Yoo K, Attal M, Walcott R. 2013. Influence of lithology on hillslope morphology and response to tectonic forcing in the northern Sierra Nevada of California. *Journal of Geophysical Research - Earth Surface* **118**: 832–851.

Hutton J. 1788. X. Theory of the earth; or an investigation of the laws observable in the composition, dissolution, and restoration of land upon the globe. *Transactions of the Royal Society of Edinburgh* **1**: 209–304.

Jackson CT. 1840. *Report on the Geological and Agricultural Survey of the State of Rhode Island*. B. Cranston and Co.: Providence, RI.

Jacobson AD, Blum J. 2003. Relationship between mechanical erosion and atmospheric CO2 consumption in the New Zealand Southern Alps. *Geology* **31**: 865–868.

Jenny H. 1941. *Factors of Soil Formation: A System of Quantitative Pedology*. McGraw-Hill Book Company: New York.

Jin L, Ravella R, Ketchum B, Bierman PR, Heaney P, White TS, Brantley SL. 2010. Mineral weathering and elemental transport during hillslope evolution at the Susquehanna/Shale Hills Critical Zone Observatory. *Geochimica et Cosmochimica Acta* **74**: 3669–3691.

Johnson DL, Domier JEJ, Johnson DN. 2005. Animating the biodynamics of soil thickness using process vector analysis: a dynamic denudation approach to soil formation. *Geomorphology* **67**: 23–46.

Johnson NM, Likens GE, Bormann FH, Pierce R. 1968. Rate of chemical weathering of silicate minerals in New Hampshire. *Geochimica et Cosmochimica Acta* **32**: 531–545.

Johnstone SA, Hilley GE. 2015. Lithologic control on the form of soil-mantled hillslopes. *Geology* **43**: 83–86.

Jones DP, Graham RC. 1993. Water-holding characteristics of weathered granitic rock in chaparral and forest ecosystems. *Soil Science Society of America Journal* **57**: 256–261.

Kelly EF, Chadwick OA, Hilinski TE. 1998. The effect of plants on mineral weathering. *Biogeochemistry* **42**: 21–53.

Knapp RB. 1989. Spatial and temporal scales of local equilibrium in dynamic fluid-rock systems. *Geochimica et Cosmochimica Acta* **53**: 1955–1964.

Kump LR, Brantley SL, Arthur MA. 2000. Chemical, weathering, atmospheric CO2, and climate. *Annual Review of Earth and Planetary Sciences* **28**: 611–667.

Kuntz BW, Rubin S, Berkowitz B, Singha K. 2011. Quantifying solute transport at the Shale Hills Critical Zone Observatory. *Vadose Zone Journal* **10**: 843–857.

Kurtz AC, Lugolobi F, Salvucci G. 2011. Germanium-silicon as a flow path tracer: Application to the Rio Icacos watershed. *Water Resources Research* **47**: 1–16. DOI:10.1029/2010WR009853.

Kurz MD. 1986. Cosmogenic helium in a terrestrial igneous rock. *Nature* **320**: 435–439.

Larsen IJ, Montgomery DR, Greenberg HM. 2014. The contribution of mountains to global denudation. *Geology* **42**: 527–530.

Lasaga AC. 1981. Rate laws of chemical reactions. In *Kinetics of Geochemical Processes*, Lasaga AC, Kirkpatrick RJ (eds). Reviews in Mineralogy and Geochemistry: Washington, DC.

Lebedeva MI, Brantley SL. 2013. Exploring geochemical controls on weathering and erosion of convex hillslopes: beyond the empirical regolith production function. *Earth Surface Processes and Landforms* **38**: 1793–1807.

Lebedeva MI, Fletcher RC, Balashov VN, Brantley SL. 2007. A reactive diffusion model describing transformation of bedrock to saprolite. *Chemical Geology* **244**: 624–645.

Lebedeva MI, Fletcher RC, Brantley SL. 2010. A mathematical model for steady-state regolith production at constant erosion rate. *Earth Surface Processes and Landforms* **35**: 508–524.

Lee VW, Mackwell SJ, Brantley SL. 1991. The effect of fluid chemistry on wetting textures in novaculite. *Journal of Geophysical Research* **96**: 10023–10037.

Leopold M, Völkel J, Huber J, Dethier DP. 2013. Subsurface architecture of the Boulder Creek Critical Zone Observatory from electrical resistivity tomography. *Earth Surface Processes and Landforms* **38**: 1417–1431.

Lerman A, Wu L. 2008. Kinetics of global geochemical cycles. In *Kinetics of Water–Rock Interaction*, Brantley SL, Kubicki JD, White AF (eds). Springer: New York; 655–736.

Li J-WW, Vasconcelos PM, Duzgoren-Aydin NS, Yan D-R, Zhang W, Deng X-D, Zhao X-F, Zeng Z-P, Hu M-A. 2007. Neogene weathering and supergene manganese enrichment in subtropical South China: an 40Ar/39Ar approach and paleoclimatic significance. *Earth and Planetary Science Letters* **256**: 389–402.

Lichtner PC. 1988. The quasi-stationary state approximation to coupled mass transport and fluid–rock interaction in a porous medium. *Geochimica et Cosmochimica Acta* **52**: 143–165.

Likens GE, Bormann FH, Johnson NM, Pierce RS. 1967. The calcium, magnesium, potassium, and sodium budgets for a small forested ecosystem. *Ecology* **48**: 772–785.

Lindberg SE, Lovett GM, Richter DD, Johnson DW. 1986. Atmospheric deposition and canopy interactions of major ions in a forest. *Science* **231**: 141–145.

Lukens CE, Riebe CS, Sklar LS, Shuster DL. 2016. Grain-size bias in cosmogenic nuclide studies of catchment-wide erosion. *Journal of Geophysical Research - Earth Surface* **121**: 978–999.

Ma L, Chabaux F, Pelt E, Blaes E, Jin L, Brantley SL. 2010. Regolith production rates calculated with uranium-series isotopes at Susquehanna/Shale Hills Critical Zone Observatory. *Earth and Planetary Science Letters* **297**: 211–225.

Ma L, Chabaux F, West N, Kirby E, Jin L, Brantley SL. 2013. Regolith production and transport in the Susquehanna Shale Hills Critical Zone Observatory, Part 1: Insights from U-series isotopes. *Journal of Geophysical Research - Earth Surface* **118**: 722–740.

Maher K, Chamberlain CP. 2014. Hydrologic regulation of chemical weathering and the geologic carbon cycle. *Science* **343**: 1502–1504.

Maher K. 2010. The dependence of chemical weathering rates on fluid residence time. *Earth and Planetary Science Letters* **294**: 101–110.

Maher K. 2011. The role of fluid residence time and topographic scales in determining chemical fluxes from landscapes. *Earth and Planetary Science Letters* **312**: 48–58.

Marini L. 2006. *Geological Sequestration of Carbon Dioxide: Thermodynamics, Kinetics, and Reaction Path Modelling*. Elsevier: Amsterdam.

Marshall CE, Haseman JF. 1942. The quantitative evolution of soil formation and development by heavy mineral studies: a Grundy silt-loam profile. *Soil Science Society of America Journal* **7**: 448–553.

Marshall JA, Roering JJ, Bartlein PJ, Gavin DG, Granger DE, Rempel AW, Praskievicz SJ, Hales TC. 2015. Frost for the trees: did climate increase erosion in unglaciated landscapes during the late Pleistocene? *Science Advances* **1**: e1500715–e1500715.

Martel SJ. 2011. Mechanics of curved surfaces, with application to surface-parallel cracks. *Geophysical Research Letters* **38**: 1–6, L20303.

Martin JM, Meybeck M. 1979. Elemental mass-balance of material carried by major world rivers. *Marine Chemistry* **7**: 173–206.

McDowell WH, Asbury CE. 1994. Export of carbon, nitrogen, and major ions from three tropical montane watersheds. *Limnology and Oceanography* **34**: 111–125.

McKean JA, Dietrich WE, Finkel RC, Southon JR, Caffee MW. 1993. Quantification of soil production and downslope creep rates from cosmogenic ^{10}Be accumulations on a hillslope profile. *Geology* **21**: 343–346.

Merriam JL, McDowell WH, Tank JL, Wollheim WM, Crenshaw CL, Johnson SL. 2002. Characterizing nitrogen dynamics, retention and transport in a tropical rainforest stream using an *in situ* ^{15}N addition. *Freshwater Biology* **47**: 143–160.

Merrill GP. 1897. *A Treatise on Rocks, Rock-weathering and Soils*. Macmillan Company: New York.

Merritts D, Chadwick OA, Hendricks DM, Brimhall GH, Jr, Lewis CJ. 1992. The mass balance of soil evolution on late Quaternary marine terraces, northern California. *Geological Society of America, Bulletin* **104**: 1456–1470.

Meybeck M. 1987. Global chemical-weathering of surficial rocks estimated from river dissolved loads. *American Journal of Science* **287**: 401–428.

Minasny B, McBratney AB. 2001. A rudimentary mechanistic model for soil formation and landscape development II. A two-dimensional model incorporating chemical weathering. *Geoderma* **103**: 161–179.

Minasny B, McBratney AB, Salvador-Blanes S. 2008. Quantitative models for pedogenesis – a review. *Geoderma* **144**: 140–157.

Molnar P, Anderson RS, Anderson SP. 2007. Tectonics, fracturing of rock, and erosion. *Journal of Geophysical Research* **112**: 1–12.

Monaghan M, McKean J, Dietrich WE, Klein J. 1992. Be-10 chronometry of bedrock-to-soil conversion rates. *Earth and Planetary Science Letters* **111**: 483–492.

Monaghan MC, Elmore D. 1994. 'Garden variety' ^{10}Be in soils on hill slopes. *Nuclear Instruments and Methods in Physics Research B* **92**: 357–361.

Montgomery DR. 2007. Is agriculture eroding civilization's foundation? *GSA Today* **17**: 4–9.

Moon S, Chamberlain CP, Blisniuk K, Levine N, Rood DH, Hilley GE. 2011. Climatic control of denudation in the deglaciated landscape of the Washington Cascades. *Nature Geoscience* **4**: 469–473.

Moore J, Lichtner PC, White AF, Brantley SL. 2012. Using a reactive transport model to elucidate differences between laboratory and field dissolution rates in regolith. *Geochimica et Cosmochimica Acta* **93**: 235–261.

Moulton K, West AJ, Berner RA. 2000. Solute flux and mineral mass balance approaches to the quantification of plant effects on silicate weathering. *American Journal of Science* **300**: 539–570.

Moulton KL, Berner RA. 1998. Quantification of the effect of plants on weathering: studies in Iceland. *Geology* **26**: 895–570.

Mudd SM, Yoo K. 2010. Reservoir theory for studying the geochemical evolution of soils. *Journal of Geophysical Research* **115**: 1–13.

Murphy S, Brantley SL, Blum AE, White AF, Dong H. 1998. Chemical weathering in a tropical watershed, Luquillo Mountains, Puerto Rico: II. Rate and mechanism of biotite weathering. *Geochimica et Cosmochimica Acta* **62**: 227–243.

Nahon DB. 1986. Evolution of iron crusts in tropical landscapes. In *Rates of Chemical Weathering of Rocks and Minerals*, Colman SM, Dethier DP (eds). Academic Press: Orlando, FL; 169–187.

National Research Council (NRC). 2001. *Basic Research Opportunities in Earth Science*. The National Academies Press: Washington, DC.

National Research Council (NRC). 2010. *Landscapes on the Edge: New Horizons for Research on Earth's Surface*. The National Academies Press: Washington, DC.

National Research Council (NRC). 2012. *New Research Opportunities in Earth Science*. The National Academies Press: Washington, DC.

Navarre-Sitchler A, Brantley SL, Rother G. 2015. How porosity increases during incipient weathering of crystalline silicate rocks. *Reviews in Mineralogy and Geochemistry* **80**: 331–354.

Nesbitt HW. 1979. Mobility and fractionation of rare-earth elements during weathering of a granodiorite. *Nature* **279**: 206–210.

Nesbitt HW, Young GM. 1982. Early Proterozoic climates and plate motions inferred from major element chemistry of lutites. *Nature* **299**: 715–717.

Nikiforoff CC, Drosdoff M. 1943. Genesis of a claypan soil I. *Soil Science* **55**: 459–482.

Nishiizumi K, Lal D, Klein J, Middleton R, Arnold JR. 1986. Production of Be-10 and Al-26 by cosmic-rays in terrestrial quartz *in situ* and implications for erosion rates. *Nature* **319**: 134–136.

Oelkers EH, Schott J. 2009. *Thermodynamics and Kinetics of Water–Rock Interaction*. Mineralogical Society of America: Chantilly, VA.

Ollier C. 1988. Deep weathering, groundwater and climate. *Geografiska Annaler, Series A, Physical Geography* **70**: 285–290.

Pačes T. 1973. Steady-state kinetics and equilibrium between ground water and granitic rock. *Geochimica et Cosmochimica Acta* **37**: 2641–2663.

Pačes T. 1983. Rate constants of dissolution derived from the measurements of mass balance in hydrological catchments. *Geochimica et Cosmochimica Acta* **47**: 1855–1863.

Pačes T. 1986. Rates of weathering and erosion derived from mass balance in small drainage basins. In *Rates of Chemical Weathering of Rocks and Minerals*, Colman SL, Dethier DP (eds). Academic Press: Orlando, FL; 531–551.

Palandri JL, Kharaka YK. 2004. *A Compilation of Rate Parameters of Water–Mineral Interaction Kinetics for Application to Geochemical Modeling*. US Department of the Interior, Geological Survey: Menlo Park, CA.

Parker A. 1970. Index of weathering for silicate rocks. *Geological Magazine* **107**: 501–504.

Parsekian AD, Singha K, Minsley BJ, Holbrook WS, Slater L. 2015. Multiscale geophysical imaging of the critical zone. *Reviews of Geophysics* **53**: 1–26.

Pavich MJ. 1986. Processes and rates of saprolite production and erosion on a foliated granitic rock of the Virginia Piedmont. In *Rates of Chemical Weathering of Rocks and Minerals*, Coleman SM, Dethier DP (eds). Academic Press: Orlando, FL; 551–590.

Pavich MJ, Brown L, Valette-Silver JN, Klein J, Middleton R. 1985. ^{10}Be analysis of a Quaternary weathering profile in the Virginia Piedmont. *Geology* **13**: 39–42.

Pawlik Ł. 2013. The role of trees in the geomorphic system of forested hillslopes — a review. *Earth-Science Reviews* **126**: 250–265.

Pelletier JD, Barron-Gafford GA, Breshears DD, Brooks PD, Chorover J, Durcik M, Harman CJ, Huxman TE, Lohse KA, Lybrand R, Meixner T, McIntosh JC, Papuga SA, Rasmussen C, Schaap M, Swetnam TL, Troch PA. 2013. Coevolution of nonlinear trends in vegetation, soils, and topography with elevation and slope aspect: a case study in the sky islands of southern Arizona. *Journal of Geophysical Research - Earth Surface* **118**: 1–18.

Peters NE. 1984. *Evaluation of Environmental Factors Affecting Yields of Major Dissolved Ions of Streams in the United States*. US Government Printing Office: Washington, DC.

Phillips FM, Leavy BD, Jannik NO, Elmore D, Kubik PW. 1986. The accumulation of cosmogenic chlorine-36 in rocks: a method for surface exposure dating. *Science* **231**: 41–43.

Phillips JD. 2009. Biological energy in landscape evolution. *American Journal of Science* **309**: 271–289.

Portenga EW, Bierman PR. 2011. Understanding Earth's eroding surface with Be-10. *GSA Today* **21**: 4–10.

Price JR, Velbel MA. 2003. Chemical weathering indices applied to weathering profiles developed on heterogeneous felsic metamorphic parent rocks. *Chemical Geology* **202**: 397–416.

Price JR, Rice KC, Szymanski DW. 2013. Mass-balance modeling of mineral weathering rates and CO2 consumption in the forested, metabasaltic Hauver Branch watershed, Catoctin Mountain, Maryland, USA. *Earth Surface Processes and Landforms* **38**: 859–875.

Rasmussen C, Tabor NJ. 2007. Applying a quantitative pedogenic energy model across a range of environmental gradients. *Soil Science Society of America Journal* **71**: 1719–1729.

Rasmussen C, Brantley SL, Richter DD, Blum AE, Dixon JL, White AF. 2011b. Strong climate and tectonic control on plagioclase weathering in granitic terrain. *Earth and Planetary Science Letters* **301**: 521–530.

Rasmussen C, Pelletier JD, Troch PA, Swetnam TL, Chorover J. 2015. Quantifying topographic and vegetation effects on the transfer of energy and mass to the critical zone. *Vadose Zone Journal* **14**: 1–16. DOI:10.2136/vzj2014.07.0102.

Rasmussen C, Southard RJ, Horwath WR. 2005. Modeling energy inputs to predict pedogenic environments using regional environmental databases. *Soil Science Society of America Journal* **69**: 1266–1274.

Rasmussen C, Troch PA, Chorover J, Brooks PD, Pelletier J, Huxman TE. 2011a. An open system framework for integrating critical zone structure and function. *Biogeochemistry* **102**: 15–29.

Raymo ME, Ruddiman WF. 1992. Tectonic forcing of late Cenozoic climate. *Nature* **359**: 117–122.

Rempe DM, Dietrich WE. 2014. A bottom-up control on fresh-bedrock topography under landscapes. *Proceedings of the National Academy of Sciences* **111**: 6576–6581.

Rempel AW, Marshall JA, Roering JJ. 2016. Modeling relative frost weathering rates at geomorphic scales. *Earth and Planetary Science Letters* **453**: 87–95.

Richardson BA, Richardson MJ, Scatena FN, McDowell WH. 2000. Effects of nutrient availability and other elevational changes on bromeliad populations and their invertebrate communities in a humid tropical forest in Puerto Rico. *Journal of Tropical Ecology* **16**: 167–188.

Richter DD, Markewitz D. 1995. How deep is soil? *BioScience* **45**: 600–609.

Richter DD, Markewitz D, Wells CG, Allen HL, April R, Heine PR, Urrego B. 1994. Soil chemical change during three decades in an old-field loblolly pine (*Pinus taeda L.*) ecosystem. *Ecology* **75**: 1463–1473.

Riebe CS, Chorover J. 2014. Report on drilling, sampling, and imaging the depths of the critical zone, an NSF Workshop. *Open Project Report to the Critical Zone Community*. National Science Foundation: Arlington, VA.

Riebe CS, Granger DE. 2013. Quantifying effects of deep and near-surface chemical erosion on cosmogenic nuclides in soils, saprolite, and sediment. *Earth Surface Processes and Landforms* **38**: 523–533.

Riebe CS, Kirchner JW, Granger DE. 2001a. Quantifying quartz enrichment and its consequences for cosmogenic measurements of erosion rates from alluvial sediment and regolith. *Geomorphology* **40**: 15–19.

Riebe CS, Kirchner JW, Granger DE, Finkel RC. 2001b. Strong tectonic and weak climatic control of long-term chemical weathering rates. *Geology* **29**: 511–514.

Riebe CS, Kirchner JW, Finkel RC. 2003. Long-term rates of chemical weathering and physical erosion from cosmogenic nuclides and geochemical mass balance. *Geochimica et Cosmochimica Acta* **67**: 4411–4427.

Riebe CS, Kirchner JW, Finkel RC. 2004. Erosional and climatic effects on long-term chemical weathering rates in granitic landscapes spanning diverse climate regimes. *Earth and Planetary Science Letters* **224**: 547–562.

Riebe CS, Sklar LS, Lukens CE, Shuster DL. 2015. Climate and topography control the size and flux of sediment produced on steep mountain slopes. *Proceedings of the National Academy of Science* **112**: 15574–15579.

Riggins SG, Anderson RS, Anderson SP, Tye AM. 2011. Solving a conundrum of a steady-state hilltop with variable soil depths and production rates, Bodmin Moor, UK. *Geomorphology* **128**: 73–84.

Rivé K, Gaillardet J, Agrinier P, Rad S. 2013. Carbon isotopes in the rivers from the Lesser Antilles: origin of the carbonic acid consumed by weathering reactions in the Lesser Antilles. *Earth Surface Processes and Landforms* **38**: 1020–1035.

Robinson DA, Binley A, Crook N, Day-Lewis FD, Ferré TPA, Grauch VJS, Knight R, Knoll M, Lakshmi V, Miller R, Nyquist J, Pellerin L, Singha K, Slater L. 2008. Advancing process-based watershed hydrological research using near-surface geophysics: a vision for, and review of, electrical and magnetic geophysical methods. *Hydrological Processes* **22**: 3604–3635.

Roelandt C, Goddéris Y, Bonnet M-P, Sondag F. 2010. Coupled modeling of biospheric and chemical weathering processes at the continental scale. *Global Biogeochemical Cycles* **24**: 1–18.

Roering JJ, Kirchner JW, Dietrich WE. 1999. Evidence for nonlinear, diffusive sediment transport on hillslopes and implications for landscape morphology. *Water Resources Research* **35**: 853–870.

Roering JJ, Marshall JA, Booth AM, Mort M, Jin Q. 2010. Evidence for biotic controls on topography and soil production. *Earth and Planetary Science Letters* **298**: 183–190.

Rogers WB, Rogers RE. 1848. On the decomposition and partial solution of minerals, rocks, etc., by pure water and water charged with carbonic acid. *American Journal of Science* **2**: 401–405.

Ruxton BP, Berry L. 1957. Weathering of granite and associated erosional features in Hong Kong. *Geological Society of America, Bulletin* **68**: 1263–1292.

Ruxton BP, Berry L. 1959. The basal rock surface on weathered granitic rocks. *Proceedings of the Geologists' Association* **70**: 285–290.

Salehikhoo F, Li L, Brantley SL. 2013. Magnesite dissolution rates at different spatial scales: the role of mineral spatial distribution and flow velocity. *Geochimica et Cosmochimica Acta* **108**: 91–106.

Salve R, Rempe DM, Dietrich WE. 2012. Rain, rock moisture dynamics, and the rapid response of perched groundwater in weathered, fractured argillite underlying a steep hillslope. *Water Resources Research* **48**: 1–25.

Scatena FN. 1989. An Introduction to the Physiography and History of the Bisley Experimental Watersheds in the Luquillo Mountains of Puerto Rico. US Department of Agriculture General Technical Report SO-72. US Department of Agriculture: New Orleans, LA; 1–22.

Shuster DL, Farley KA, Vasconcelos PM, Balco G, Monteiro HS, Waltenberg K, Stone JOH. 2012. Cosmogenic ^{3}He in hematite and goethite from Brazilian 'canga' duricrust demonstrates the extreme stability of these surfaces. *Earth and Planetary Science Letters* **329–330**: 41–50.

Shuster DL, Vasconcelos PM, Heim JA, Farley KA. 2005. Weathering geochronology by (U-Th)/He dating of goethite. *Geochimica et Cosmochimica Acta* **69**: 659–673.

Slim M, Perron JT, Martel SJ. 2015. Topographic stress and rock fracture: a two-dimensional numerical model for arbitrary topography and preliminary comparison with borehole observations. *Earth Surface Processes and Landforms* **40**: 512–529.

Small EE, Anderson RS, Hancock GS. 1999. Estimates of the rate of regolith production using Be-10 and Al-26 from an alpine hillslope. *Geomorphology* **27**: 131–150.

St. Clair J, Moon S, Holbrook WS, Perron JT, Riebe CS, Martel SJ, Carr B, Harman C, Singha K, Richter DD. 2015. Geophysical imaging reveals topographic stress control of bedrock weathering. *Science* **350**: 534–538.

Stallard RF. 1985. River chemistry, geology, geomorphology, and soils in the Amazon and Orinoco basins. In *The Chemistry of Weathering*, Drever JI (ed). D. Reidel Publishing Company: Dordrecht; 293–316.

Stallard RF, Edmond JM. 1983. Geochemistry of the Amazon 2. The influence of geology and weathering environment on the dissolved load. *Journal of Geophysical Research* **88**: 9671–9688.

Steefel CI, DePaolo DJ, Lichtner P. 2005. Reactive transport modeling: an essential tool and a new research approach for the Earth sciences. *Earth and Planetary Science Letters* **240**: 539–558.

Stefansson A, Gíslason SR. 2001. Chemical weathering of basalts, southwest Iceland: effect of rock crystallinity and secondary minerals on chemical fluxes to the ocean. *American Journal of Science* **301**: 513–556.

Stonestrom DA, White AF, Akstin KC. 1998. Determining rates of chemical weathering in soils--solute transport versus profile evolution. *Journal of Hydrology* **209**: 331–345.

Sverjensky DA. 1992. Linear free energy relations for predicting dissolution rates of solids. *Nature* **358**: 310–313.

Swoboda-Colberg NG, Drever JI. 1993. Mineral dissolution rates in plot-scale field and laboratory experiments. *Chemical Geology* **105**: 51–69.

Taylor AB, Velbel MA. 1991. Geochemical mass balances and weathering rates in forested watersheds of the southern Blue Ridge II. Effects of botanical uptake terms. *Geoderma* **51**: 29–50.

Taylor HP. 1974. The application of oxygen and hydrogen isotope studies to problems of hydrothermal alteration and ore deposition. *Economic Geology* **69**: 843–883.

Thomas MF. 1966. Some geomorphological implications of deep weathering patterns in crystalline rocks in Nigeria. *Transactions of the Institute of British Geographers* **40**: 173–193.

Tipper E, Bickle MJ, Galy A, West AJ, Pomiès C, Chapman HJ. 2006. The short term climatic sensitivity of carbonate and silicate weathering fluxes: insight from seasonal variations in river chemistry. *Geochimica et Cosmochimica Acta* **70**: 2737–2754.

Tóth J. 1963. A theoretical analysis of groundwater flow in small drainage basins. *Journal of Geophysical Research* **68**: 4795–4812.

Turner BF, Stallard RF, Brantley SL. 2003. Investigation of *in situ* weathering of quartz diorite bedrock in the Rio Icacos basin, Luquillo Experimental Forest, Puerto Rico. *Chemical Geology* **202**: 313–341.

Urey HC. 1952. *The Planets, Their Origin and Development*. Yale University Press: New Haven, CT.

Vasconcelos PM, Conroy M. 2003. Geochronology of weathering and landscape evolution, Dugald River valley, NW Queensland, Australia. *Geochimica et Cosmochimica Acta* **67**: 2913–2930.

Vasconcelos PM, Renne PR, Brimhall GH, Jr, Becker TA. 1994. Direct dating of weathering phenomena by Ar-40/Ar-39 and K-Ar analysis of supergene K-Mn oxides. *Geochimica et Cosmochimica Acta* **58**: 1635–1665.

Velbel MA. 1985. Geochemical mass balances and weathering rates in forested watersheds of the southern Blue Ridge. *American Journal of Science* **285**: 904–930.

Velbel MA. 1986. The mathematical basis for determining rates of geochemical and geomorphic processes in small forested watersheds by mass balance: examples and implications. In *Rates of Chemical Weathering of Rocks and Minerals*, Colman SM, Dethier DP (eds). Academic Press: Orlando, FL; 439–449.

Velbel MA. 1993. Constancy of silicate-mineral weathering-rate ratios between natural and experimental weathering: implications for hydrologic control of differences in absolute rates. *Chemical Geology* **105**: 89–99.

Velbel MA, Price JR. 2007. Solute geochemical mass-balances and mineral weathering rates in small watersheds: methodology, recent advances, and future directions. *Applied Geochemistry* **22**: 1682–1700.

von Blanckenburg F. 2005. The control mechanisms of erosion and weathering at basin scale from cosmogenic nuclides in river sediment. *Earth and Planetary Science Letters* **237**: 462–479.

Wald JA, Graham RC, Schoeneberger PJ. 2013. Distribution and properties of soft weathered bedrock at ≤1 m depth in the contiguous United States. *Earth Surface Processes and Landforms* **38**: 614–626.

Waldbauer JR, Chamberlain CP. 2005. Influence of uplift, weathering, and base cation supply on past and future CO_2 levels. In *A History of Atmospheric CO_2 and Its Effects on Plants, Animals, and Ecosystems*, Ehleringer JR, Cerling T, Dearing MD (eds). Springer: New York; 166–184.

Walder J, Hallet B. 1985. A theoretical model of the fracture of rock during freezing. *Geological Society of America, Bulletin* **96**: 336–346.

Walker JCG, Hays PB, Kasting JF. 1981. A negative feedback mechanism for the long-term stabilization of the Earth's surface temperature. *Journal of Geophysical Research* **86**: 9776–9782.

West AJ. 2012. Thickness of the chemical weathering zone and implications for erosional and climatic drivers of weathering and for carbon-cycle feedbacks. *Geology* **40**: 811–814.

West AJ, Galy A, Bickle MJ. 2005. Tectonic and climatic controls on silicate weathering. *Earth and Planetary Science Letters* **235**: 211–228.

West N, Kirby E, Bierman PR, Slingerland R, Ma L, Rood D, Brantley SL. 2013. Regolith production and transport at the Susquehanna Shale Hills Critical Zone Observatory, Part 2: Insights from meteoric ^{10}Be. *Journal of Geophysical Research - Earth Surface* **118**: 1877–1896.

White AF. 1995. Chemical weathering rates of silicate minerals in soils. *Reviews in Mineralogy and Geochemistry* **31**: 407–461.

White AF. 2002. Determining mineral weathering rates based on solid and solute weathering gradients and velocities: application to biotite weathering in saprolites. *Chemical Geology* **190**: 69–89.

White AF. 2008. Quantitative approaches to characterizing natural chemical weathering rates. In *Kinetics of Water–Rock Interaction*, Brantley SL, Kubicki JD, White AF (eds). Springer: New York; 469–543.

White AF, Blum AE. 1995. Effects of climate on chemical weathering in watersheds. *Geochimica et Cosmochimica Acta* **59**: 1729–1747.

White AF, Brantley SL. 2003. The effect of time on the weathering of silicate minerals: why do weathering rates differ in the laboratory and field? *Chemical Geology* **202**: 479–506.

White AF, Blum AE, Bullen TD, Vivit DV, Schulz M, Fitzpatrick JA. 1999a. The effect of temperature on experimental and natural chemical weathering rates of granitoid rocks. *Geochimica et Cosmochimica Acta* **63**: 3277–3291.

White AF, Blum AE, Schultz MS, Bullen TD, Harden JW, Peterson ML. 1996. Chemical weathering rates of a soil chronosequence on granitic alluvium: I. Quantification of mineralogical and surface area changes and calculation of primary silicate reactions. *Geochimica et Cosmochimica Acta* **60**: 2533–2550.

White AF, Blum AE, Schulz MS, Vivit DV, Stonestrom DA, Larsen MC, Murphy SF, Eberl D. 1998. Chemical weathering in a tropical watershed, Luquillo Mountains, Puerto Rico: I. Long-term versus short-term weathering fluxes. *Geochimica et Cosmochimica Acta* **62**: 209–226.

White AF, Bullen TD, Schulz MS, Blum AE, Huntington TG, Peters NE. 2001. Differential rates of feldspar weathering in granitic regoliths. *Geochimica et Cosmochimica Acta* **65**: 847–869.

White AF, Bullen TD, Vivit DV, Schulz MS. 1999b. The role of disseminated calcite in the chemical weathering of granitoid rocks. *Geochimica et Cosmochimica Acta* **63**: 1939–1953.

White AF, Schulz MS, Stonestrom DA, Vivit DV, Fitzpatrick JA, Bullen TD. 2008. Solute profiles in soils, weathering gradients and exchange equilibrium/disequilibrium. *Mineralogical Magazine* **72**: 149–153.

Wilkinson MT, Chappell J, Humphreys GS, Fifield K, Smith B, Hesse PP. 2005. Soil production in heath and forest, Blue Mountains, Australia: influence of lithology and palaeoclimate. *Earth Surface Processes and Landforms* **30**: 923–934.

Willenbring JK, von Blanckenburg F. 2010. Meteoric cosmogenic Beryllium-10 adsorbed to river sediment and soil: Applications for Earth-surface dynamics. *Earth-Science Reviews* **98**: 105–122.

Yoo K, Amundson RC, Heimsath AM, Dietrich WE, Brimhall GH, Jr. 2007. Integration of geochemical mass balance with sediment transport to calculate rates of soil chemical weathering and transport on hillslopes. *Journal of Geophysical Research* **112**: 1–15.

Yoo K, Mudd SM, Sanderman J, Amundson RC, Blum AE. 2009. Spatial patterns and controls of soil chemical weathering rates along a transient hillslope. *Earth and Planetary Science Letters* **288**: 184–193.

Zanner CW, Graham RC. 2005. Deep regolith: exploring the lower reaches of soil. *Geoderma* **126**: 1–3.

Zhang PZ, Molnar P, Downs WR. 2001. Increased sedimentation rates and grain sizes 2-4 Myr ago due to the influence of climate change on erosion rates. *Nature* **410**: 891–897.

Zhu C. 2005. *In situ* feldspar dissolution rates in an aquifer. *Geochimica et Cosmochimica Acta* **69**: 1435–1453.